La mer 40 : 161–170, 2002
Société franco-japonaise d'océanographie, Tokyo

Lower Trophic Level Ecosystem in Jakarta Bay, Indonesia

Nurdjaman SUSANNA* and Tetsuo YANAGI**

Abstract : The lower trophic level ecosystem of Jakarta Bay, Indonesia in wet and dry seasons is studied by using observed data and a box ecosystem model. The observed values of chlorophyll-*a* and Dissolved Inorganic Nitrogen (DIN) concentration are well reproduced by a vertical one-dimensional ecosystem model except in wet season 1976. Chlorophyll-*a* and DIN concentrations are higher in wet season than in dry season. Generally, concentrations of ecosystem compartments are higher in wet season than in dry season. Rainfall directly affects on the growth of phytoplankton in Jakarta Bay and the primary production in Jakarta Bay (416–830 mgC/m^2/day) is larger than in Banten Bay (84–122 mgC/m^2/day; SUSANNA and YANAGI, 2002). According to primary production Jakarta Bay is classified under mesotrophic and Banten Bay is oligotrophic. In Banten Bay, the regenerated production is higher than the new production and plays an important role, while in Jakarta Bay the ratio of new production to regenerated production is almost one. Both nutrient load and recycling DIN play an important role in the increasing of chlorophyll-*a* concentration in Jakarta Bay.

Keywords : *Jakarta Bay, DIN, chlorophyll-a, box ecosystem model, primary production, Banten Bay.*

1. Introduction

Jakarta Bay is a semi-enclosed bay, and is connected to the Java Sea. This area is directly affected by human activities because it is close to the large city, Jakarta, which is one of the fast growing Asian mega-cities that have sprung up during the past few decades. As the urbanization and industrial activities extend, the nutrient supply has increased. The waters of Jakarta Bay are fed by several major coastal rivers, which transport sediments and sewage water, as well as agricultural and industrial effluents (Fig.1). This has resulted in high levels of nutrients concentration and in the contamination of coastal waters extending for a considerable distance into the Java Sea. In recent years, a severe water pollution accompanied with red tides and oxygen-depleted water mass has been frequently observed in Jakarta Bay. These phenomena are said to be related to the increase in the coastal nutrient supply. High nutrients level can lead to enhanced phytoplankton growth and potentially to eutrophication. Repeated observations in Jakarta Bay revealed that the bay water is very productive. The averaged chlorophyll-*a* concentration ranged from 0.9 to 5.41 mg/m^3 with a maximum value of 17.96 mg/m^3 (PRASENO *et al.,* 1978). The highest chlorophyll-*a* concentration was found in the sample taken in front of the river mouth. Blooming of a single species was observed in Jakarta Bay by Praseno and ADNAN (1978). The plankton *Noctiluca* was often found blooming in waters influenced by river discharge, appearing in great numbers after the heavy rainfall.

There are many studies concerning the coastal marine ecosystem and many attempts to estimate the environmental management strategy (SOHMA *et al.*, 2001). Simulation by numerical model is one of tools that can be used to predict the management effect quantitatively.

FASHAM *et al.* (1990) presented a model of the annual cycle of plankton dynamics and

* Interdisiplinary Graduate School of Engineering Sciences, Kyushu University, Kasuga 816-8580, Japan
** Research Institute for Applied Mechanics, Kyushu University, Kasuga 816-8580, Japan

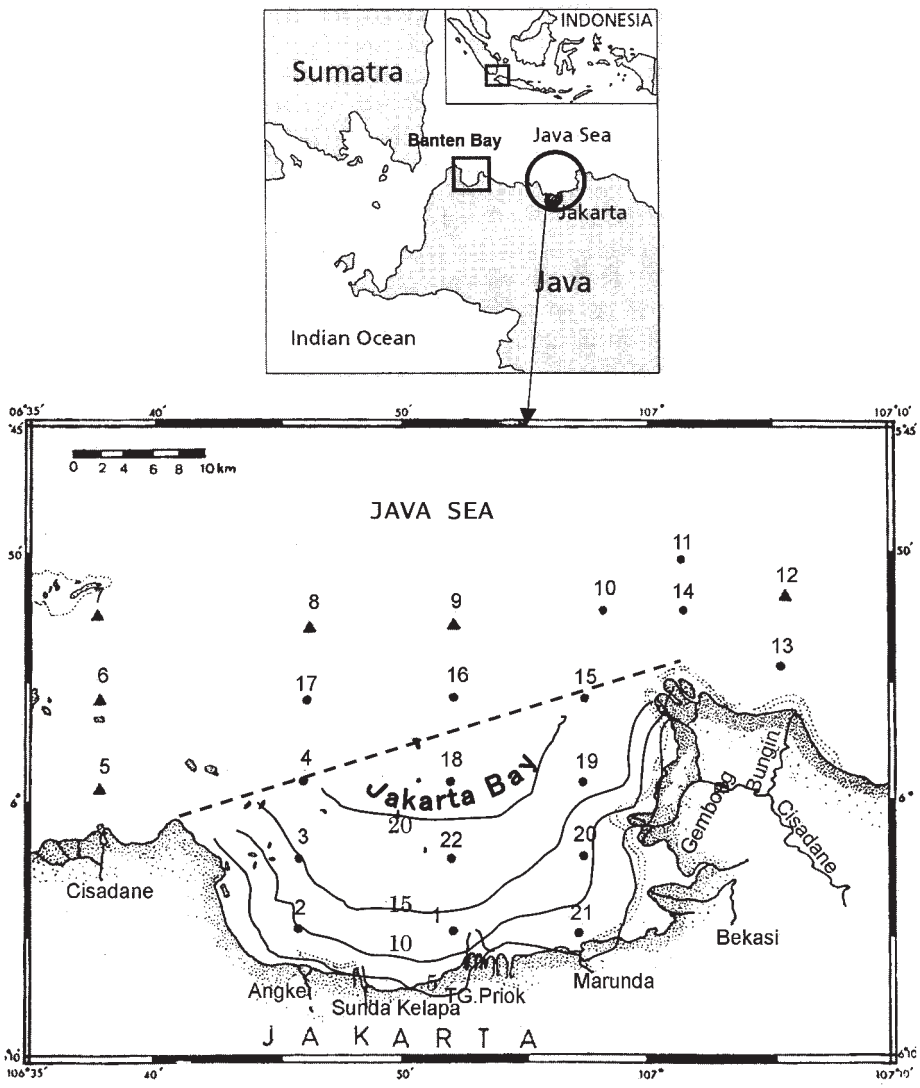

Fig. 1 Jakarta Bay and observation stations. Numbers with contour show the depth in meters. Broken line shows the model boundary.

nitrogen cycling in the oceanic mixed layer at Station "S" near Bermuda. KAWAMIYA *et al.* (1995) also developed a model which has constructed a vertical one-dimensional ecosystem and applied to Station Papa.

In this paper, a box ecosystem model has been described that reproduces the observation field, using the best available parameters. An application of the model has been a calculation of detailed budget of bioelement through the coastal ecosystem. The results are compared with the previous estimate of nutrient fluxes in Banten Bay (SUSANNA and YANAGI, 2002), which is located next to Jakarta Bay (Fig.1) to assess the performance of the model and to identify which process requires a detailed study.

2. Observation

Research and Development Center for Oceanology of the Indonesia carried out field observations at 22 stations shown in Fig. 1

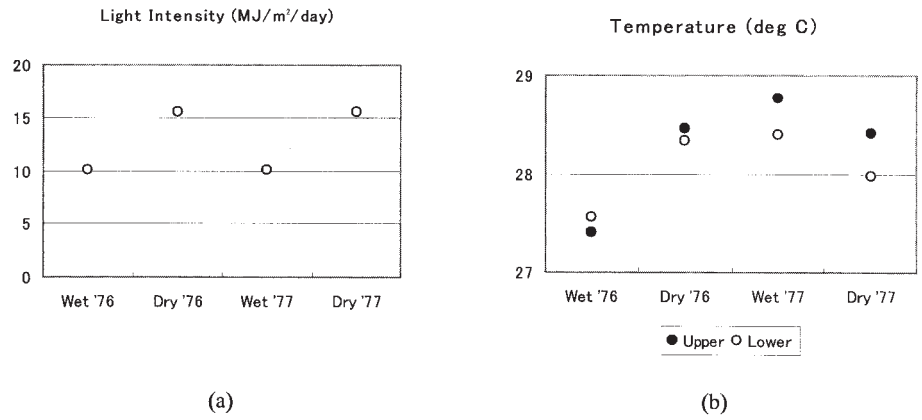

Fig. 2 Seasonal variation of light intensity at Jakarta (a) and average water temperatures in the upper and lower layers of Jakarta Bay (b).

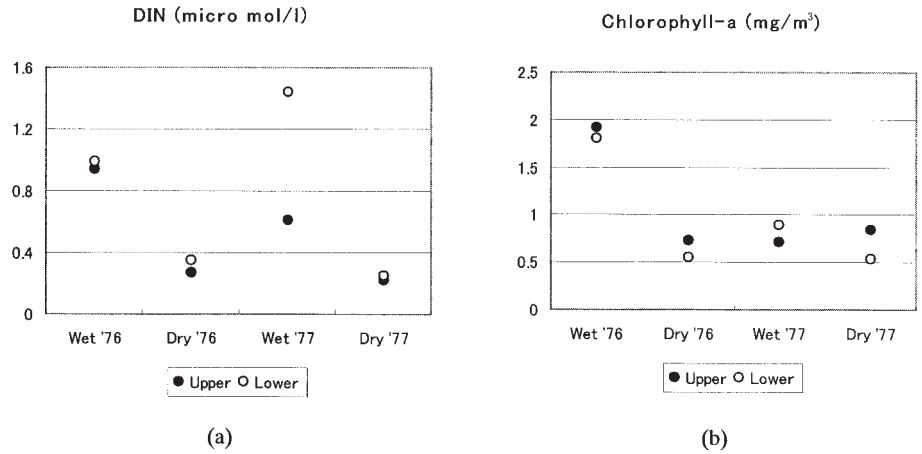

Fig. 3 Seasonal variation of DIN concentration (a) and chlorophyll-*a* concentration (b) at outer bay.

during 1976 to 1977. Samplings were carried out during both wet and dry seasons, and they were 21–23 January 1976 (wet season), 10–12 August 1976 (dry season), 26–29 January 1977 (wet season) , and 10–13 August 1977 (dry season). The field observations of water temperature, dissolved inorganic nitrogen (DIN) and chlorophyll-*a* concentrations were taken at the depths of 0, 5, 10, 15, 20... meters. The data of stations 5 to 14, 16 and 17 are used as outer values (boundary condition of the model) and those of stations 1 to 4, 15, 18, 19, 20, 21 and 22 as inner values (for verification). Seasonal variation of solar radiation (I) at Jakarta was observed by Geophysics and Meteorology Agency, Indonesia (Fig. 2 (a)). The thickness of the euphotic layer (H_u) is taken to be 7.0 m in wet season and 10.0 m in dry season, on the basis of the sechi disk depth data in the bay (ANONYMOUS, 1976 a, b, 1977 a, b). Euphotic depth is 2.8 times the Sechi disk depth (PARSONS *et al.*, 1984). Variation of water temperature in the upper (euphotic) and lower (aphotic) layers are shown in Fig. 2(b). Estimation of land effect on water temperature in Jakarta Bay showed that there was convection of heat energy from land to sea water (ILAHUDE and SIANIPAR, 1977). Besides, water temperature near river mouth was higher than other sites in Jakarta Bay in January 1977

(wet season) (ILAHUDE and SOEPANGAT, 1977). Concentrations of DIN and chlorophyll-*a* at outer bay are used for the boundary conditions of the model calculation (Fig. 3).

The average load of DIN from rivers, industrial and sewage treatment plants, which flow into Jakarta Bay, is estimated to be 305.8 g/sec in wet season and 235.8 g/sec in dry season (ANONYMOUS, 1997c).

3. Model Description

We consider that the simplest model capable of capturing the essence of nitrogen cycling requires five compartments. These compartments are: Phytoplankton (PHY), Zooplankton (ZOO), Particulate Organic Nitrogen (PON), Dissolved Organic Nitrogen (DON) and DIN. The structure of nitrogen based material flows are described by SUSANNA and YANAGI (2002). All compartments of ecosystem are applied in the upper (euphotic) and lower (aphotic) layers. Major flows include nitrogen uptake by phytoplankton, excretion, ingestion, grazing, mortality and decomposition of particulate materials. While bacteria plankton is not modeled explicitly, their effects are modeled indirectly through the decomposition and cycling of organic substances from the senescent cells of phytoplankton and zooplankton. The dynamics of each compartment are described with differential equations, which are composed of biological source and sink terms, and diffusion terms. Details are given below (based on KAWAMIYA *et al*,. 1995) :

$$\frac{d\mathrm{PHY}}{d\mathrm{t}} = -w_p\mathrm{PHY} + Diffusion(\mathrm{PHY}) + (A_1\mathrm{PHY} - B_1\mathrm{ZOO} - A_2\mathrm{PHY} - A_3\mathrm{PHY}^2) \quad (1)$$

$$\frac{d\mathrm{ZOO}}{d\mathrm{t}} = Diffusion(\mathrm{ZOO}) + (B_1\mathrm{ZOO} - B_2\mathrm{ZOO} - B_3\mathrm{ZOO} - B_4\mathrm{ZOO}^2) \quad (2)$$

$$\frac{d\mathrm{PON}}{d\mathrm{t}} = -w_D\,\mathrm{PON} + Diffusion(\mathrm{PON}) + (A_3\mathrm{PHY}^2 + B_3\mathrm{ZOO} + B_4\mathrm{ZOO}^2 - C_1\mathrm{PON} - C_2\mathrm{PON}) \quad (3)$$

$$\frac{d\mathrm{DON}}{d\mathrm{t}} = Diffusion(\mathrm{DON}) + (A_2\mathrm{PHY} + C_2\mathrm{PON} - D_1\mathrm{DON}) \quad (4)$$

$$\frac{d\mathrm{DIN}}{d\mathrm{t}} = Diffusion(\mathrm{DIN}) + (-\mathrm{A}_1\mathrm{PHY} + B_2\mathrm{ZOO} + C_1\mathrm{PON} + D_1\mathrm{DON}) \quad (5)$$

where $Diffusion(C_i)$ is vertical and horizontal diffusion of C_i (one of the compartment concentration in this model). Vertical diffusion is $\frac{\partial}{\partial z}\left(K_v\frac{\partial C_i}{\partial z}\right)$ and horizontal diffusion is $\frac{\partial}{\partial x}\left(K_h\frac{\partial C_i}{\partial x}\right)$, where K_v and K_h denote the vertical and horizontal eddy diffusivities. Horizontal diffusivity (K_h) is 13 m^2/sec and vertical diffusivity (K_v) = 2.0×10^{-4} m^2/sec are decided based on SUSANNA and YANAGI (2002). w_P and w_D denote the sinking velocity of phytoplankton and PON, respectively.

The following are explanation of biochemical formulations.

a. Photosynthesis (A_1)

Photosynthesis is assumed to be a function of temperature, nutrient concentration and light intensity. The Michaelis-Menten equation is used to define the nutrient limited growth rate (FASHAM *et al.*, 1983). As for the dependence on light intensity, the formula used by STEELE (1962), by which light inhibition can be expressed, is employed.

$$A_1 = V_{max}\left(\frac{DIN_u}{DIN_u + K_N}\right).exp(kT_u).\frac{I_a}{I_{opt}}exp\left(1-\frac{I_a}{I_{opt}}\right), \quad (6)$$

where V_{max} is the maximum nitrogen uptake rate, K_N is a half saturation constant for DIN, k denotes the temperature dependency of photosynthesis, T_u is temperature in the upper layer, I_{opt} is optimum light intensity for photosynthesis and I_a is average light intensity in the upper layer :

$$I_a = \frac{1}{H_u}\int_0^{H_u} 0.5Iexp(-k_e z)\,dz, \quad (7)$$

where 0.5 is the conversion factor for the fraction of photosynthetically active radiation in the total radiation (PARSONS *et al.*, 1984), I is the total surface radiation observed at Jakarta (shown in Fig. 2a) and k_e is the extinction coefficient as estimated by $k_e = 4.6/H_u$, where H_u is the thickness of the euphotic layer (PARSONS *et al.*, 1984).

b. Extracellular Excretion (A_2)

Table 1 Parameter values used in this model. Values in parentheses are those used by KAWAMIYA *et al.* (1995).

V_{max}	Maximum photosynthesis rate at 0℃	1.3(1.0)	/day
K	Temperature coefficient for Photosynthesis rate	0.063	/℃
K_N	Half Saturation constant for dissolve inorganic nitrogen	0.98(3.0)	μmol/l
I_{opt}	Optimum Light Intensity	18.0(4.21)	MJ/m^2/day
γ	Ratio of Extra cellular Excretion to Photosynthesis	0.135	
M_{PO}	Phytoplankton Mortality Rate at 0℃	0.0281	1/μmolN day
k_{MP}	Temperature Coefficient fot Phytoplankton Mortality rate	0.069	/℃
α	Assimilation Efficiency of Zooplankton	0.7	
β	Growth Efficiency of Zooplankton	0.3	
GR_{max}	Maximum Grazing Rate at 0℃	0.3	/day
k_g	Temperature Coefficient for Grazing	0.0693	/℃
λ	Ivlev Constant	1.4	1/μmolN
PHY	Threshold Value for Grazing	0.043	μmolN/l
M_{ZO}	Zooplankton Mortality Rate at 0℃	0.0585	1/μmolN day
k_{MZ}	Temperature Coefficient for Zooplankton Mortality rate	0.0693	/℃
V_{PIO}	PON Decomposition Rate at 0℃(to DIN)	0.03	/day
V_{PIT}	Temperature Coefficient for PON Decomposition(to DIN)	0.0693	/℃
V_{PDO}	PON Decomposition Rate at 0℃(to DIN)	0.03	/day
V_{PDT}	Temperature Coefficient for PON Decomposition(to DIN)	0.0693	/℃
V_{DIO}	DON Decomposition Rate at 0℃	0.03	/day
V_{DIT}	Temperature Coefficient for DON Decomposition	0.0693	/℃
w_p	Sinking speed of phytoplankton	0.037(0.05)	m/day
w_D	Sinking speed of detritus	0.38 (0.5)	m/day

Extracellular excretion is the fraction of net primary production exuded by phytoplankton as DON (GIN *et al.*, 1998), which is assumed to be proportional to photosynthesis (KAWAMIYA *et al.*, 1995).

$$A_2 = \gamma A_1 \quad (8)$$

where γ r is phytoplankton exudation rate.

c. Mortality (A_3, B_4)

Following STEELE and HENDERSON (1992), mortality of phytoplankton and zooplankton is assumed to be proportional to the second power of plankton concentration and dependent on temperature.

$$\text{Mortality of phytoplankton}(A_3) = M_{PO}\, exp\,(k_{MP}T) \quad (9)$$

$$\text{Mortality of zooplankton}(B_4) = M_{ZO}\, exp\,(k_{MZ}T) \quad (10)$$

where M_{po} *and* M_{zo} are mortality rates of phytoplankton and zooplankton at 0℃, respectively. The dead plankton forms the organic nitrogen pools (PON, DON) and are subject to mineralization by bacteria to form DIN. In order to keep the model simple, a linear decay function is used, instead of introducing a separate bacterial compartment.

d. Grazing (B_1)

Grazing process is assumed to be as a function of temperature, phytoplankton concentration and zooplankton concentration.

$$B_1 = G_{max}(1 - exp(\lambda\,(PHY^* - PHY)) \cdot exp(k_g T) \quad (11)$$

where G_{max} refers to maximum grazing rate, λ is Ivlev's constant, PHY^* is a threshold value for grazing, k_g is temperature coefficient for grazing, and T is water temperature. Grazing rate is saturated when phytoplankton concentration is sufficiently large, while no grazing occurs when phytoplankton concentration is lower than the critical value PHY^*.

e. Excretion and Egestion (B_2, B_3)

Excretion and egestion are assumed to be proportional to grazing rate.

$$\text{Excretion}(B_2) = (\alpha - \beta) B_1 \quad (12)$$

$$\text{Egestion}(B_3) = (1 - \alpha)\, B_1 \quad (13)$$

where α and β are assimilation efficiency

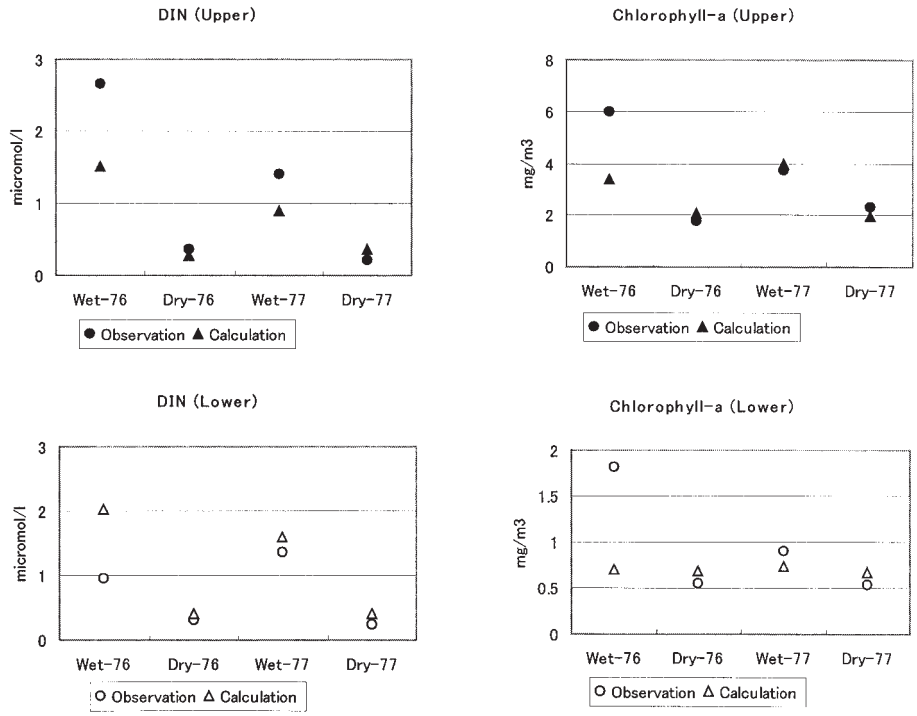

Fig. 4 Comparison between calculated and observed values for DIN and chlorophyll-*a* concentrations in Jakarta Bay.

and growth efficiency of zooplankton, respectively.

f. Decomposition of Organic Matters (C_1, C_2, D_1)

Decomposition of PON into DIN(C_1) =

$$V_{PIO}\ exp\ (V_{PIT}T) \quad (14)$$

Decomposition of PON into DON(C_2) =

$$V_{PDO}\ exp\ (V_{PDT}T) \quad (15)$$

Decomposition of DON into DIN(D_1) =

$$V_{DIO}\ exp\ (V_{DIT}T) \quad (16)$$

where V_{PI0}, V_{PD0}, V_{DI0} are decomposition rates at 0℃, V_{PIT}, V_{PDT}, V_{DIT} are temperature coefficients.

Parameters used in this box model analysis are shown in Table 1.

According to Parsons *et al.* (1984), the range of photosynthetic rate (V_{max}) is 0.05 /day − 8.1/day, and 1.3 /day (at 0℃) is adopted in this model. Larger V_{max} than by KAWAMIYA *et al.*, (1995) may be due to that their model was applied to Station Papa which is in the open ocean or oligotrophic condition. For the half saturation constant of DIN (KN), PARSONS *et al.* (1984) shows that the range is 0.01 − 4.21 mmol/l, and 0.98 mmol/l was reported for eutrophic tropical Pacific (PARSONS *et al.*, 1984). Such small K_N in tropics is considered to be due to that DIN concentration in tropics is much lower than that in mid-latitude.

The initial condition is given as the same values as those at outer bay (Fig. 3). The quasi-steady state is obtained 50 days after the beginning of the calculation. As the horizontal gradient terms are much larger than the temporal changing terms in equations (1) to (5), we consider the quasi-steady state is established in each observation time.

4. Results and Discussion

a. Comparison with observed data

Fig. 4 shows the seasonal variations of calculated and observed DIN and chlorophyll-*a* in Jakarta Bay. Calculated chlorophyll-*a* and DIN concentrations well reproduces the observed values in the upper and lower layers of Jakarta Bay except in wet season 1976. Concentration

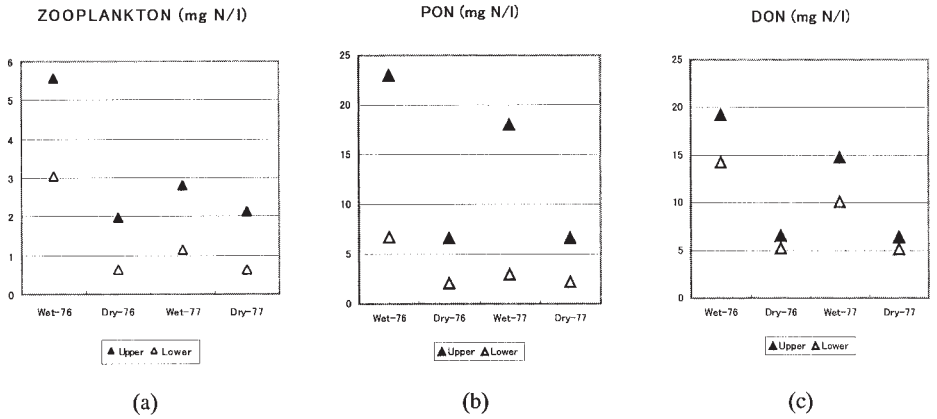

Fig. 5 Results of calculated zooplankton, PON and DON concentrations in Jakarta Bay.

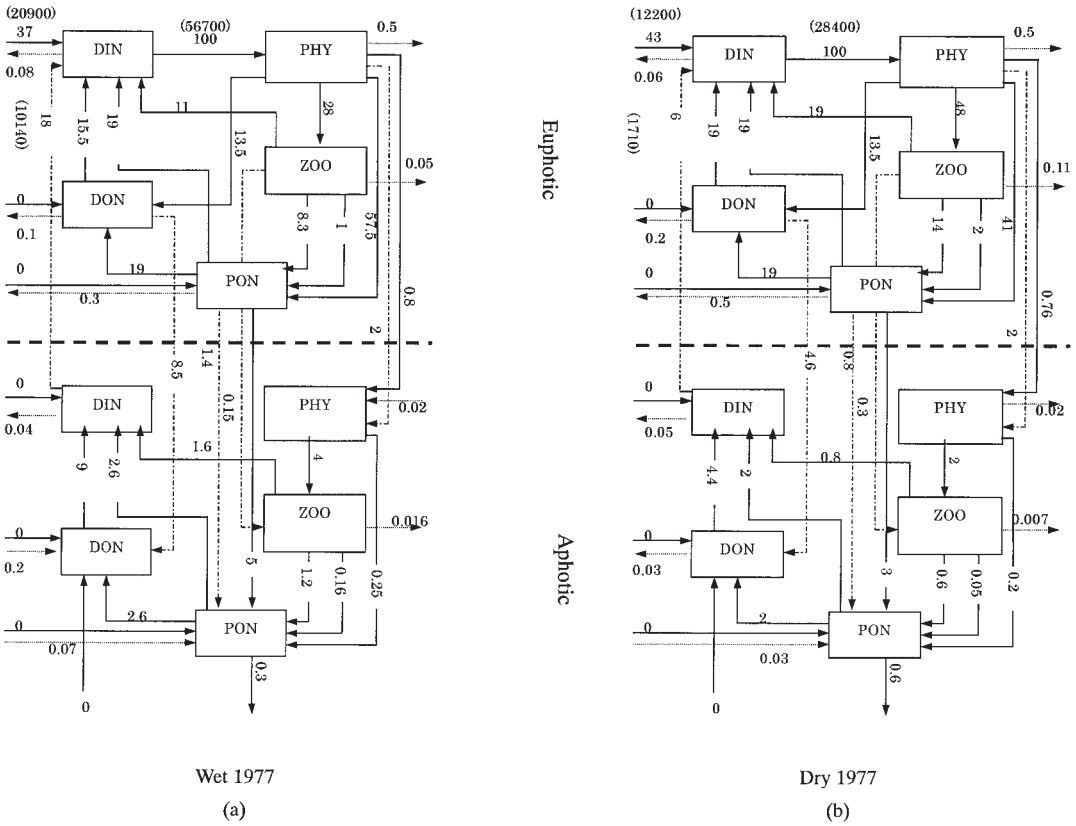

Fig. 6 Normalized nitrogen flux based on the photosynthesis flux in January 1977 (wet season) (a) and August 1977 (dry season) (b) in Jakarta Bay (unit in kg/day)

of chlorophyll-*a* in Jakarta Bay is higher in wet season than in dry season. From model results, chlorophyll-*a* concentration in the lower layer seems to show little seasonal variation. The discrepancy in wet season 1976 in DIN concentration is due to the insufficiency of data for DIN load each year, that is, only averaged DIN load data are given in this model.

Table 2 Comparison of average ecosystem conditions between Jakarta Bay and Banten Bay during wet and dry seasons.

		Jakarta Bay		Banten Bay	
		Way 1977	Dry 1977	Wet 1979	Dry 1980
DIN (microg/l)	upper	1.40	0.20	1.19	0.23
	lower	1.44	0.23	1.25	0.30
Chl-a (mg/m^3)	upper	3.93	2.29	0.79	0.95
	lower	0.89	0.53	0.65	0.86
Nitrogen Flux					
DIN-Phy(kg/day)		56700	28400	2220	3220
Load(kg/day)		20900	12200	63	21
New Production (kg/day)		31100	14000	460	430
Regenerated Prod. (kg/day)		25800	16300	1770	2730
Ratio new production /regenerated prod.		1:0.8 (1.25)	1:1.2 (0.80)	1:3.9 (0.26)	1:6.3 (0.15)
Primary production (mg C/m^2/day)		830	416	83.9	122
Secondary production (mg C/m^2/day)		231	199	15.4	25.3
Transfer Efficiency(%)		28	48	18	21

Calculated DIN concentration is higher in wet season than in dry season, because the load from river is larger in wet season than in dry season. Rainfall played an important role on the growth of phytoplankton and nutrient concentration, which is higher during the northwest monsoon (wet season) (ARINARDI, 1978).

Fig. 5 shows the variation in zooplankton, PON and DON. Generally, all the concentrations are higher in wet season than in dry season. This pattern is related to chlorophyll-*a* and DIN concentrations, being higher in wet season than in dry season.

b. Nitrogen Cycling

Nitrogen flux (Fig. 6) from DIN to phytoplankton is higher in wet season (56,700 kgN/day) than in dry season (28,400 kg N/day). Such a flux difference is caused by higher chlorophyll-*a* concentration in wet season than in dry season. The inflowed DIN flux from land in wet season (20,900 kg/day) is higher than in dry season (12,200 kg/day). It means that large DIN load from land causes high chlorophyll-*a* concentration in Jakarta Bay. The ratio of inflowed DIN flux to photosynthesis-DIN flux is 2.7 in wet season and 2.3 in dry season.

From model results, seasonal variation of new production and regenerated production can be estimated. New production, which is defined as DIN flux in the upper layer from rivers or rain (load) and from the lower layer by diffusion, is larger in wet season (31,100 kgN/day) than in dry season (14,000 kgN/day) due to higher river load. Besides the vertical diffusion is also larger in wet season than in dry season. Regenerated production, which is defined as DIN flux in the upper layer by decomposition of PON and DON and excretion of zooplankton, is larger in wet season (25,800 kgN/day), when the primary production is large, than in dry season (16,300 kgN/day). The ratio of new production to regenerated production is 1: 0.8 in wet season and 1:1.2 in dry season. It means that new production is higher than regenerated production in wet season. The higher new production in wet season is due to the increasing of load from

river and the diffusion from the lower layer, while in dry season, the nutrient load is small and regenerated production plays more important role. The transfer efficiency from the primary production to the secondary production is 28 % in wet season and 48 % in dry season.

c. Comparison with Banten Bay.

DIN and chlorophyll-*a* concentrations in Jakarta Bay during wet season are higher than in Banten Bay (SUSANNA and YANAGI, 2002) (Table 2). In both bays, the values of DIN concentrations in the upper and lower layers do not have great differences. They are 1.19–1.44 μg/l in wet season and 0.20–0.30 μg/l in dry season. On the other hand, the values of chlorophyll-*a* concentration in both bays are not the same especially in the upper layer. The range of chlorophyll-*a* concentration in the upper layer is 2.29 3.93 mg/m^3 in Jakarta Bay, while in Banten Bay it has low concentration with the range of 0.79–0.95 mg/m^3. In Jakarta Bay chlorophyll-*a* concentration is higher in wet season than in dry season while in Banten Bay it is higher in dry season than in wet season. In Jakarta Bay, the rise of chlorophyll–*a* concentration in wet season is due to high rainfall and large nutrient load, but in Banten Bay, the nutrient load from river is so small that the chlorophyll-*a* concentration does not rise in wet season. Ratio of new production to regenerated production in Jakarta Bay is higher than in Banten Bay, which is over 0.8 in Jakarta Bay and under 0.26 in Banten Bay. In Jakarta Bay, high nutrient load makes the ratio of new production to regenerated production to balance, however, in Banten Bay, regenerated production is dominant due to small nutrient load and high water temperature. The primary production ranges from 416 to 830 mgC/m^2/day in Jakarta Bay and 84 to 122 mgC/m^2/day in Banten Bay. RYTHER (1969) estimates that the primary production is 137 mgC/m^2/day for the open ocean and 822 mgC/m^2/day for the coastal upwelling area and HINGA *et al.* (1995) classified the waters by the rate of organic carbon production: oligotrophic (< 274 mgC/m^2/day), mesotrophic (275–824 mgC/m^2/day), eutrophic (825–1370 mg C/m^2/day) and hyperthropic (>1370 mg C/m^2/day). According to RYTHER (1969) and HINGA *et al.* (1995), Banten Bay is oligotrophic condition (similar to the open ocean) and Jakarta Bay is mesotrophic condition.

5. Conclusion

The model calculation in Jakarta Bay shows good agreement with the observed ones except in wet season 1976. Chlorophyll-*a* concentration is higher in wet season than in dry season. The variation pattern of chlorophyll-*a* concentration coincides with that DIN concentration. High load of nutrient from industry, domestic and rainfall causes DIN concentration higher in wet season than in dry season. Generally, concentrations of lower trophic level ecosystem compartments are higher in wet season than in dry season in Jakarta Bay. This study shows that Jakarta Bay water is strongly affected by the seasonal variation.

Rainfall and recycling DIN play an important role in the increase of chlorophyll-*a* concentration. The primary production in Banten Bay is smaller than that in Jakarta Bay. According to the primary production level, Banten Bay is oligotrophic and Jakarta Bay is mesotrophic.

The box ecosystem model presented here still has limits. One of these is that the deposit materials at the bottom and release from the sediment have not been taken into account. However, as a whole, we find that a relatively simple box ecosystem model can reproduce the biochemical data at both sites.

References

ANONYMOUS (1976 a): Laporan Pelayaran II KM. Samudra di Teluk Jakarta 21–23 Januari 1976. Proyek Penelitian Masalah Pengembangan Sumber Daya Laut dan Pencemaran Laut LON LIPI, Jakarta. 1–42.

ANONYMOUS (1976 b): Laporan Pelayaran IV KM Samudera di Teluk Jakarta 10–12 Agustus 1976. Proyek Penelitian Masalah Pengembangan Sumber Daya Laut dan Pencemaran Laut LON LIPI, Jakarta. 1–40.

ANONYMOUS (1977 a): Monitoring Teluk Jakarta Laporan No. 6 Pelayaran KM. Samudera 26–29 Januari 1977. Proyek Penelitian Masalah Pengembangan Sumber Daya Laut dan Pencemaran Laut LON– LIPI, Jakarta. 1–49.

ANONYMOUS (1977 b): Pemonitoran Teluk Jakarta Laporan No. 8 Pelayaran KM. Samudra 10–13 Agustus 1977. Proyek Penelitian Masalah

Pengembangan Sumber Daya Laut dan Pencemaran Laut LON– LIPI, Jakarta. 1–57.

ANONYMOUS (1997c) : Pemantauan Kimiawi Air Sungai 1996/1997, Laporan Prokasih DKI Jakarta.

ARINARDI, O.H. (1978) : Rainfall impact on the growth of phytoplankton in Jakarta Bay 1978, Oseanologi di Indonesia, 103–120.

FASHAM, M.J.R., H.W. DUCLOW, and S.M. MCKERVIE (1990) : A Nitrogen–based model of plankton dynamics in the oceanic mixed layer, Journal of Marine Research, **48**, 591–639.

GIN, K.Y.H., J. GUO, and H. CHEONG (1998): A size based ecosystem model for pelagic waters, Ecological Modelling, **112**, 53–72.

HINGA, K.R., H. JEON, N.F. LEWIS (1995): Quantifying the effects of Nitrogen Enrichment on Phytoplankton in Coastal Ecosystems, Marine Eutrophication Review, US Dept. of Commerce, Coastal Ocean Office.

ILAHUDE, A.G., and P. SIANIPER (1977): Pengamatan hidrologi di Teluk Jakarta, Monitoring Teluk Jakarta. Laporan No. 7 Pelayaran KM 'Samudera' 11–14Mei 1977. LON–LIPI, Jakarta: 9–47.

ILAHUDE, A.G., and I. SOEPANGAT (1977): Pengamatan hidrologi di Teluk Jakarta, Monitoring Teluk Jakarta. Laporan No. 6 Pelayaran KM 'Samudera' 26–29 Januari 1977. LON–LIPI, Jakarta: 8–41.

KAWAMIYA, M., M. Kishi, Y. YAMANAKA and N. SUGINOHARA (1995) : An ecological–physical coupled model applied to Station Papa. J. Oceanography, **51**, 635–664.

PARSONS, T., M. TAKAHASHI and B. HARGRAVE (1984): Biological Oceanographic Process. Pergamon Press. 3rd edition. Oxford, 330 pp.

PRASENO, D.P., and Q. ADNAN (1978): Noctiluca miliaris Suriray in Jakarta Bay, Oseanologi di Indonesia, **11**, 1–25 (in Indonesian).

PRASENO, D.P., Z. SOEJOETI, and DIJARDJANA (1978): The application of remote semsing in marine research in Indonesia.Proc. 12th Intern. Symp. Rem. Son. Environ., **3**, 2071–2079.

RYTHER, J.H., (1969) : Photosynthesis and fish production in the sea, Science, 166, 72–76.

SOHMA, A., Y. SEKIGUCHI, H. YAMADA, T. SATO, and K. NAKATA (2001): A new coastal marine ecosystem model study coupled with hydrodynamic and tidal flat ecosystem effect, *Mar. Pollution. Bull.*, **43**, 187–208.

SUSANNA, N. and T. YANAGI (2002): Ecosystem condition in wet and dry seasons of Banten Bay, Indonesia, La mer, **40**, 1–10.

STEELE, J.H., (1962): Environmental control of photosyuthesis in sea, Limnol. Oceanogr., **7**, 137–150.

STEELE, J.H., and HENDERSON, E.W. (1992): The significance of internanuall variability. *In*: Evans, G.T., Fasham, M.J.R (Eds.), Towards a Model of Ocean Biogeochemical Processess. Springer Verlag, Heidelberg, 227–260.

Received June 17, 2002
Accepted October 15, 2002

La mer 40 : 171–182, 2002
Société franco-japonaise d'océanographie, Tokyo

The Formation of Thick and Stable Warm Eddies inside the Large Meander of the Kuroshio South of Honshu, Japan

Yoichi MAEKAWA*, Makoto UCHIDA*, Shozo YOSHIDA** and Yutaka NAGATA**

Abstract : During the period from January 2000 to October 2001, the Kuroshio was flowing in a large meandering south of Honshu, Japan. However, the flow pattern was changeable both in time and space. Two warm eddies both having a long lifetime of about 200 days were observed inside the meandering Kuroshio path, which is usually occupied by a cold-water mass (Large Cold Water Mass). XBT observations conducted on board of the R/V Seisui-maru showed that these eddies had a thick structure of several hundreds meters. Such thick and stable warm eddies have scarcely been reported in the past, except for a report by MINAMI (1989). The evolution of the abnormal warm eddies were analyzed by using the Prompt Report of Oceanic Status in the Sea off Sagami Bay and near the Izu Islands, which is published weekly by the Service Division of the Marine Information Research Center, JHA. It was shown that both warm eddies were generated from a warm-water tongue extending westward from a kink in the Kuroshio off the Izu Peninsula.

Keywords : *warm eddy, Large Meander of the Kuroshio, kink of the Kuroshio path, warm-water tongue, Enshu-nada*

1. Introduction

The Kuroshio has two stable paths while flowing along the south of Honshu, Japan: a straight path and a large meander path (e.g. SHOJI 1972 and TAFT, 1972). Both of the flow patterns are stable and are maintained for several months to several years after being established. In the case of the meandering path, the Kuroshio flows around the Large Cold Water Mass generated off Kumano-nada and/or Enshu-nada (see Fig. 1 for the place names cited in this paper). The usual evolution of a large meander of the Kuroshio is as follows: the meander is generated abruptly to the southeast of the Kii Peninsula (e.g. SHOJI, 1972, KAWABE, 1980, FUJITA *et al.*, 1998 and NAGATA *et al.*, 1999a), and stays for a considerable time as mentioned above. In the last stage, the eastern edge of the meander (or the eastern edge of the cold-water mass) shifts eastward, and after it passes the Izu-Mariana Ridge, the meander decays gradually (e.g. SHOJI, 1972). Other flow types of the path pattern have been discussed and defined by various investigators (e.g., KOBAYASHI *et al.*, 1986, KASAI *et al.*, 1993), however, except for the two basic patterns, the other patterns have a relatively short lifetime.

The Kuroshio took the large meander pattern in January 1999, and the meandering path was maintained until the end of October 2001, but the flow pattern was very changeable in time and space. The patterns, which have been thought to be transient, were often sustained for several months. Warm eddies were often generated inside of Large Cold Water Mass off Enshu-nada. Two of them had a stable nature, and persisted for about 200 days.

Intrusions of the warm Kuroshio Water into Large Cold Water Mass region have often been reported by various investigators (e.g. TAKEUCHI, 1989, MINAMI, 1989, KIMURA and SUGIMOTO, 1990, KASAI *et al.*, 1993, and SEKINE and OKUBO, 2000). However, except for the warm eddy reported off Enshu-nada by

* Training/Research Vessel Seisui-maru, Faculty of Bioresources, Mie University, 2072-2 Takanoo-cho, Tsu, Mie, 514-2221, Japan
** Marine Information Research Center, Japan Hydrographic Association, 7-15-4 Ginza, Chuo-ku, Tokyo, 104-0061, Japan

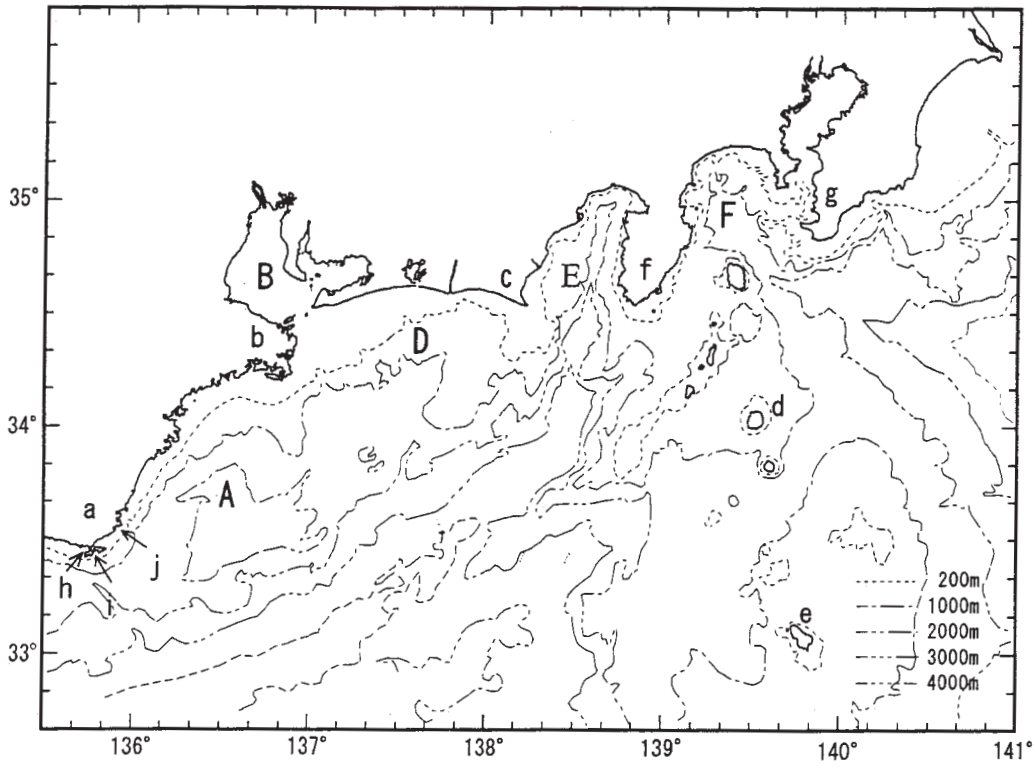

Fig. 1 Names of the locations referred to in this paper: A is the Kumano-nada, B Ise Bay, D the Enshu-nada, E Suruga Bay, F Sagami Bay, and a is the Kii Peninsula (Cape Shionomisaki is the tip of the Kii Peninsula), b Cape Daio, c Cape Omaezaki, d Miyake Island, e Hachijo Island, f the Izu Peninsula, g the Boso Peninsula, h Kushimoto, i Cape Shionomisaki, and j Uragami. Depth contours are also given for several depths.

MINAMI (1989) in 1984, these warm eddies have been shown to have a short lifetime of less than a few weeks, and structurally they were confined to the surface layer shallower than 100 m depth (TAKEUCHI, 1989, and SEKINE and OKUBO, 2000). The warm eddy found by MINAMI (1989) had a thick structure, and the eddy could be identified at least up to the depth of 400 m.

In order to evaluate the vertical structure of the two warm eddies found in 2000 and 2001, we carried out 4 surveys using R/V Seisui-maru of the Mie University to detail the temperature structure of the stable warm eddies. Also, we analyzed the time evolution of the warm eddies by using the Prompt Report of Oceanic Status in the Sea off Sagami Bay and near the Izu Islands, published weekly by the Service Division of the Marine Information Research Center, JHA.

2. Data and materials used

The Service Division of the Marine Information Research Center, JHA publishes weekly the Prompt Report of Oceanic Status in the Sea off Sagami Bay and near the Izu Islands (we shall to refer to this report as the Prompt Report, hereafter). The Prompt Report is compiled by using oceanic data collected by the Hydrographic Department of Japan Coast Guard, and by analyzing the NOAA satellite infrared image, TOPEX/POSEIDON sea level distribution which is provided on a near-real-time base by the Colorado Center for Astrodynamics Research of Colorado University (MAEKAWA *et al.*, 2001), sea level data along the coast, and so on. The Prompt Report

Table 1 List of the warm eddies observed in the period from January 2000 to December 2001. Time of generation indicates the edited date of the Prompt Report in which the isolated warm eddy was first found. Time of disappearance indicates that the warm eddy disappeared. Location of initial path kink is the place where the kink of the current path of the Kuroshio occurred prior to the generation of the warm eddy. See the text for the definition of reinforcement.

No.	time of generation	time of disappearance	period of continuation	initial location of the path kink	reinforcement
I	Feb. 9, 2000	Feb. 17, 2000	9 days	138° E	
II	Mar. 23, 2000	Sep. 21, 2000	183 days	south of Izu Peninsula(139° E)	Jun. 1, 2000
III	Nov. 23, 2000	Dec. 21, 2000	29 days	east of Kii Peninsula(137° E)	
IV	Jan. 18. 2001	Aug. 23, 2001	218 days	south of Izu Peninsula(139° E)	Apr. 19 and Jun. 7, 2001
V	Sep. 20, 2001	Oct. 25, 2001	15〜36 days	south of Izu Peninsula(139° E)	
VI	Dec. 26, 2001	Jan. 17, 2002	23 days	138〜139° E	

Table 2 XBT observations conducted on board R/V Seisui-maru. The positions of XBT observations are shown. The name of each observation run is shown in the uppermost row, and the date of the observation is shown in the second row. The numbers in the first column are the station numbers.

	XBT 1	XBT 2	XBT 3	XBT 4	XBT 5	XBT 6
date / Sta. #	Aug. 21, 2000	Aug. 30, 2000	Nov. 09, 2001	Jan. 12, 2001	Jan. 30, 2001	Mar. 05–06, 2001
1	34–15.1N 137–00.09E	33–08.35N 136–02.13E	32–59.84N 137–01.01E	34–20.04N 137–19.96E	34–20.02N 137–07.83E	33–34.52N 136–01.48E
2	34–05.00N 137–00.10E	33–14.99N 136–15.38E	33–10.02N 136–59.91E	34–15.07N 137–29.93E	34–10.00N 137–14.26E	33–34.97N 136–10.00E
3	33–55.02N 137–00.01E	33–24.00N 136–31.78E	33–19.93N 137–00.02E	34–10.01N 137–40.01E	33–59.99N 137–20.00E	33–35.13N 136–19.99E
4	33–45.02N 136–59.99E	33–31.94N 136–45.62E	33–29.92N 136–59.98E	34–05.05N 137–50.05E	34–00.01N 137–30.06E	33–35.06N 136–30.00E
5	33–34.99N 137–00.04E	33–41.03N 137–00.57E	33–39.97N 136–59.92E	34–00.19N 138–00.06E	34–00.02N 137–40.03E	33–35.06N 136–40.00E
6	33–25.49N 137–00.18E	33–45.92N 137–10.66E	33–50.40N 137–00.17E	34–00.02N 138–10.04E	33–00.01N 137–50.04E	33–35.11N 136–49.97E
7		33–50.40N 137–19.99E	33–59.97N 137–00.47E	33–59.97N 138–20.08E	33–00.00N 138–00.04E	33–35.00N 137–00.00E
8		33–56.63N 137–30.31E	34–10.00N 136–59.83E	34–00.06N 138–30.25E	34–00.00N 138–10.04E	33–45.02N 137–00.16E
9		34–00.50N 137–40.30E			34–00.05N 138–20.02E	33–55.20N 137–00.37E
10		34–04.50N 137–50.00E			34–04.21N 138–30.00E	34–05.18N 136–59.90E
11		34–09.75N 138–00.21E				34–15.25N 136–59.97E

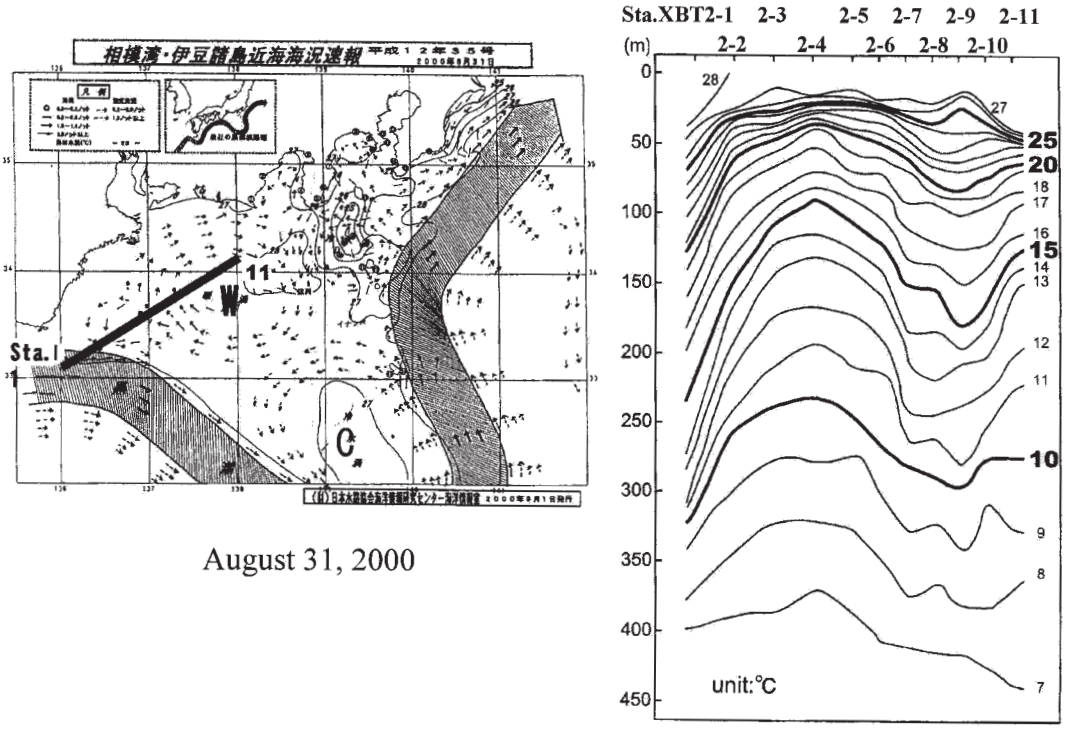

Fig. 2 Temperature cross-section along the observation line XBT2 taken on August 30, 2000 (right figure). Isotherms are given at intervals of 1 ℃, and the station names (see Table 1 for their positions) are given above the upper margin. The position of the observation line is given in the left figure together with the Prompt Report No. 35, 2000 edited on August 31. W and C indicate the warm eddy and the cold eddy (cold-water mass), respectively.

was used to monitor the warm eddies in order to determine the navigation route for the R/V Seisui-maru.

The Prompt Report was also used to determine the duration of the warm eddies inside the Kuroshio Large Meander off Enshu-nada and off Kumano-nada, and their time evolution. The warm eddies found in the period from January 2000 to December 2001 are listed in Table 1.

The R/V Seisui-maru of the Mie University was sent a total of 6 times to the area under consideration on ways to or back from the scheduled observation sites, and made XBT observations as shown in Table 2. Among these cruises, the ship course run outside of the warm eddy in the first cruise, XBT1, and the observation XBT3 was conducted at a time when no conspicuous warm eddy occurred inside the Kuroshio Large Meander. So, the observational results of these cruises will not be discussed in this paper.

3. Occurrence of the warm eddy inside the Kuroshio Large Meander in 2000-2001

Warm eddy was observed 6 times during the period from January 2000 to December 2001 as listed in Table 1. Among these eddies, Warm Eddy III (Roman numerals correspond to those in Table 1), and Warm Eddy VI are not so conspicuous and the period of continuation might be overestimated. Warm Eddy I was relatively small but conspicuous. This eddy traveled quickly around the Large Cold Water Mass and disappeared after being absorbed into the Kuroshio just off Cape Shionomisaki. Judging from this nature, the eddy would have had a relatively shallow structure and been carried counter-clockwise around the Large Cold Water Mass. We tried to find a signature of the

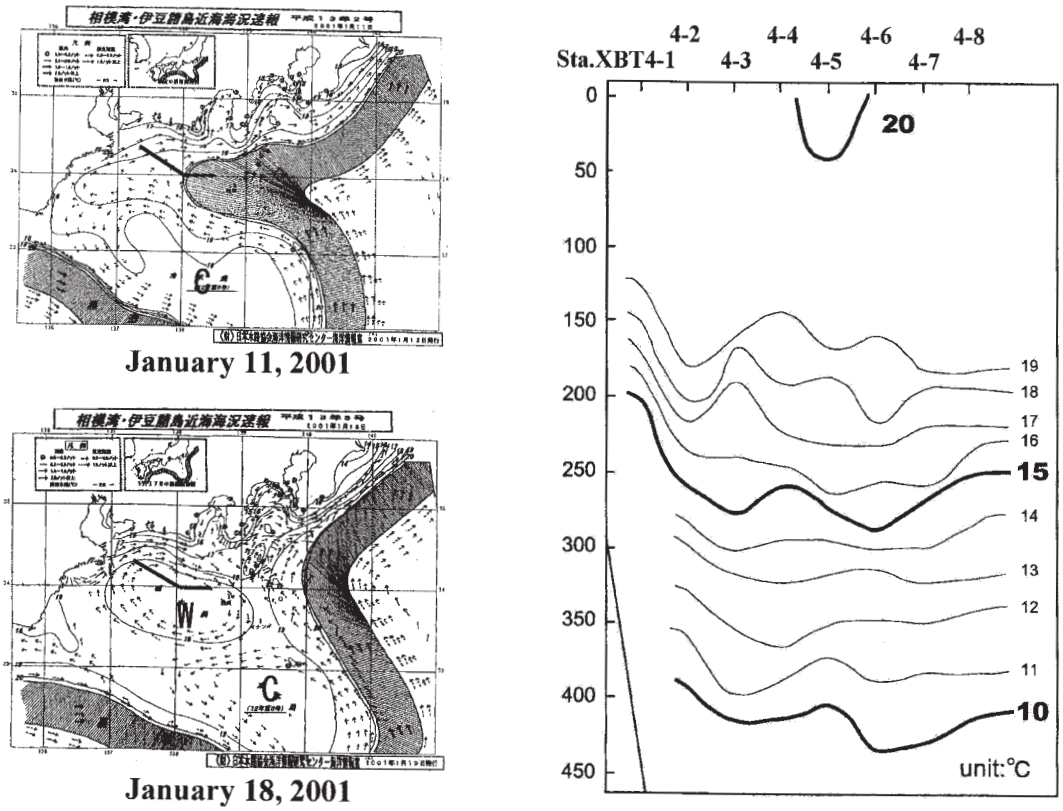

Fig. 3 The same as in fig.2, but for together with the Prompt Report No. 2 edited on January 11 (upper left figure) and No. 3 edited on January 18 (lower left figure).

warm eddies in the TOPEX/POSEIDON sea level distribution which is provided on a near-real-time base by the Colorado Center (MAEKAWA *et al.*, 2001), but no signature was found corresponding to these warm eddies. These warm eddies are considered to have had a similar nature to those reported by various investigators (TAKEUCHI, 1989, KIMURA and SUGIMOTO, 1990, KASAI *et al.*, 1993, and SEKINE and OKUBO, 2000).

In general, a kink in the current path of the Kuroshio occurred before the generation of the warm eddies. The warm-water tongue, which extended from the kink of the current path, penetrated into the cold-water region. The initial position of the kink of the Kuroshio path is shown for each warm eddy in Table 1. The warm eddies with a short lifetime were generated from kinks occurring just to the east of Cape Shionomisaki (the tip of the Kii Peninsula) or at the eastward flowing outer margin of the large meander. On the other hand warm eddies with a long lifetime, *i.e.*, Warm Eddy II and Warm Eddy IV were initiated from kinks just off the Izu Peninsula. The warm eddy with a thick structure reported by MINAMI (1989) was generated just off the Izu Peninsula. Warm Eddy V was also generated at the same position, but its period of continuation was relatively short. This might be attributed to the change of the flow pattern from the meandering path to the straight path, which occurred in October 2001.

4. The vertical structure of the stable warm eddies.

4-1. Temperature cross-section across Warm Eddy II

XBT observations of Warm Eddy II were conducted on August 30, 2000 (XBT2: see Table

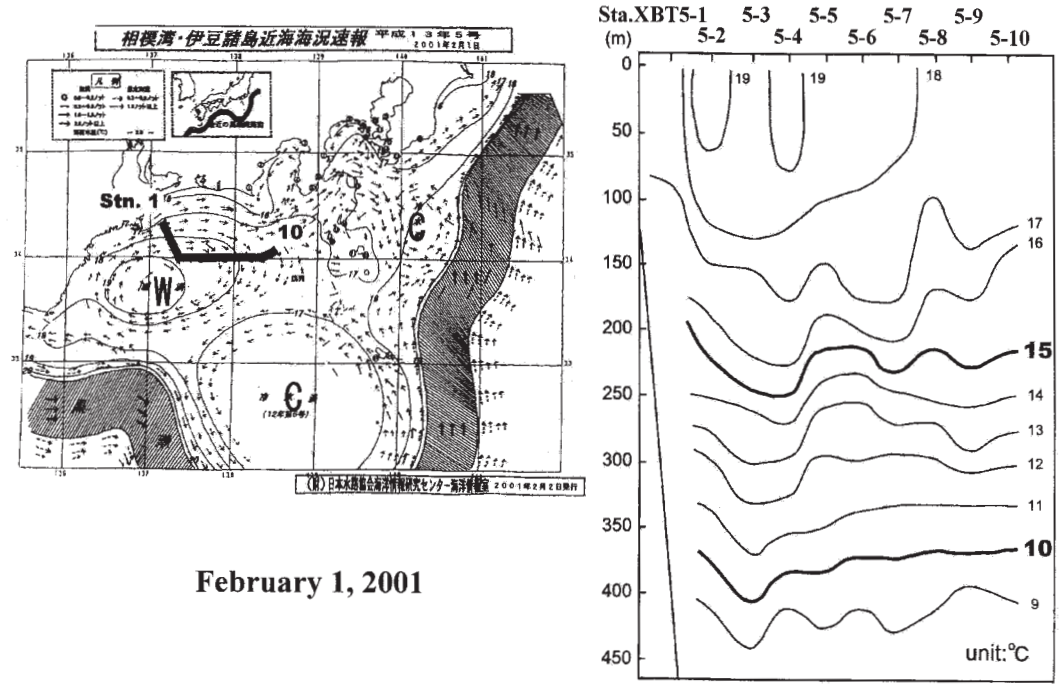

Fig. 4 The same as in Fig. 2 but for XBT5 together with Prompt Report No. 5, 2001 edited on February 1, 2001.

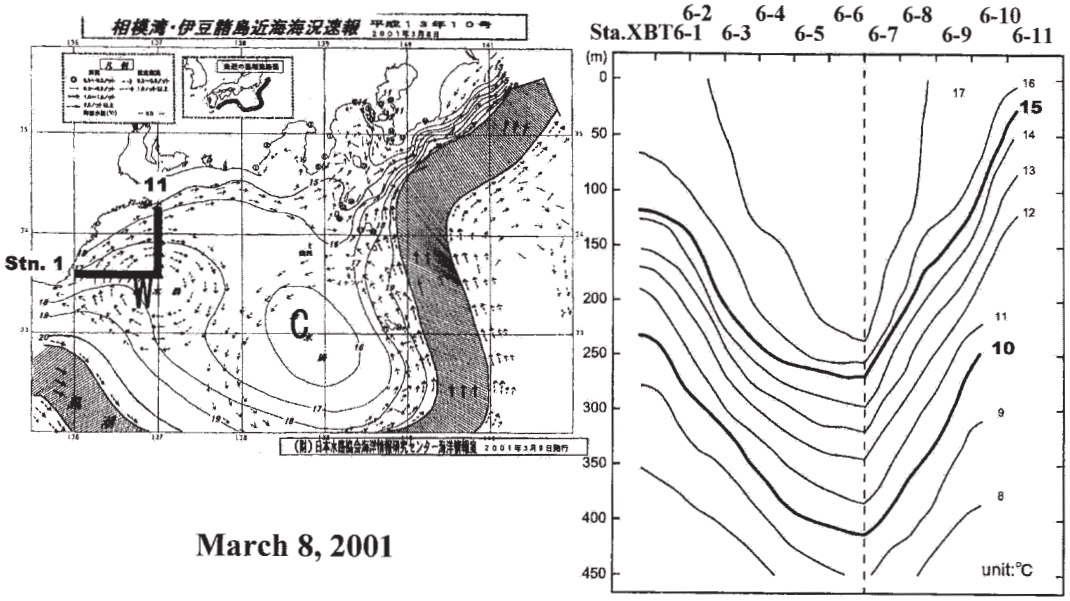

Fig. 5 The same as in Fig. 2 but for XBT6 together with Prompt Report No. 10, 2001 edited on March 8, 2001.

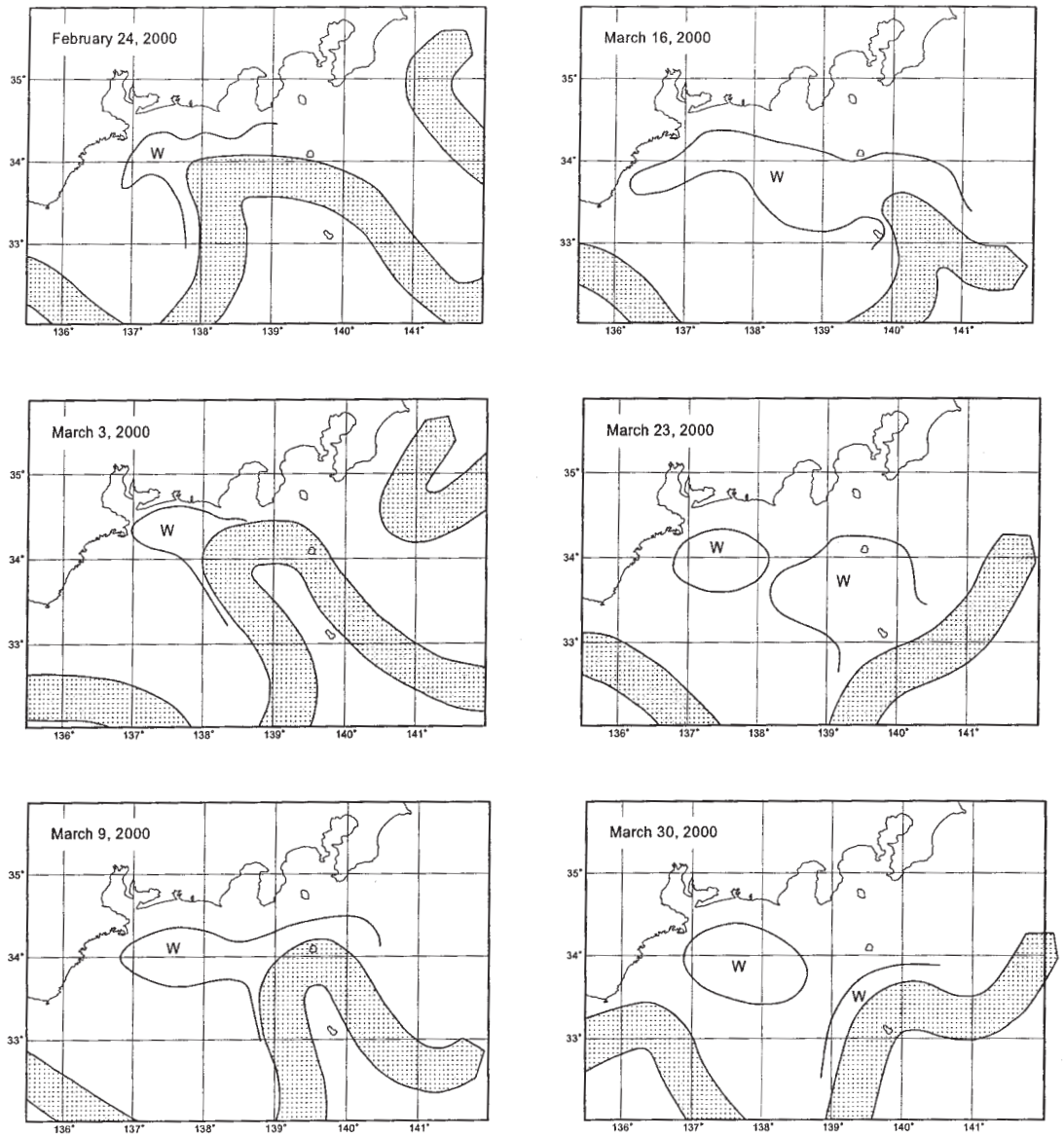

Fig. 6 Evolution of the oceanic state for the generation stage of Warm Eddy II. The current path of the Kuroshio is indicated with a hatched band, and the edges of the relatively warm water areas are shown with bold line. The distributions are derived from the Prompt Reports edited on the date shown in each figure. W indicates the warm eddy or warm area.

2). The observation line of XBT2 is shown with a bold line on the Prompt Report No. 35 edited on August 31 (left figure of Fig. 2: the Prompt Report is usually issued one or two days after its edition, and we show the date of edition here), and the temperature cross-section along the line is shown in the right figure of Fig. 2. The warm eddy is clearly seen off Enshu-nada at the time of the observation.

The sharp temperature gradient between Sta. XBT2-1 and Sta. XBT2-3 corresponds to the current zone of the Kuroshio. Warm Eddy

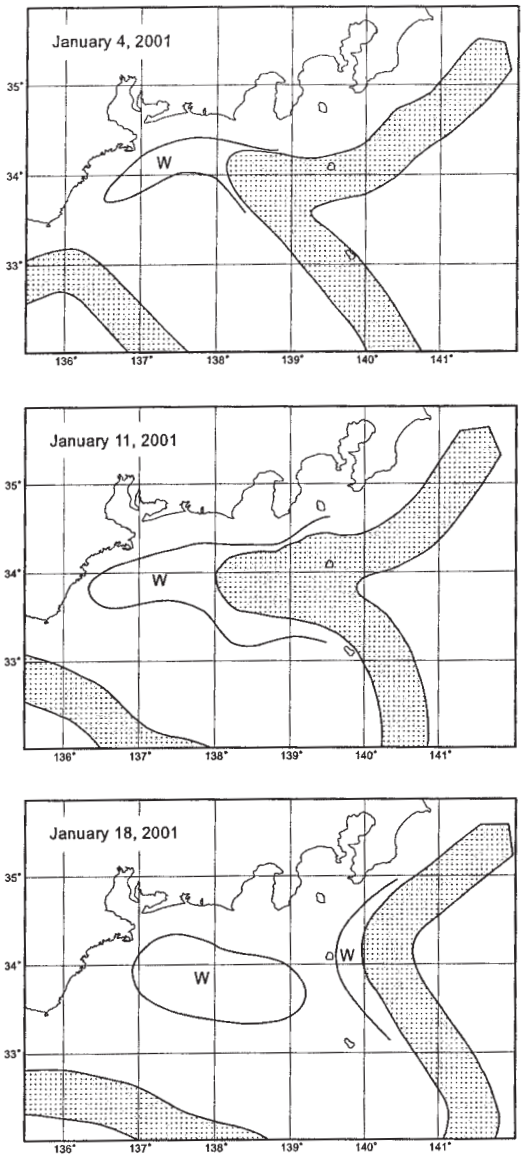

Fig. 7 The same as in Fig. 6 but for Warm Eddy IV.

II is seen between Sta. XBT2-6 and Sta. XBT2-11 as a depression of isotherms below 23 ℃. The depression is recognized to a depth of 300 m or more. Though the observation line may not pass through the center of Warm Eddy II (left figure of Fig. 2), the observed results indicate that Warm Eddy II had a considerably deep structure.

4-2. Temperature structure of Warm Eddy IV

We found a conspicuous kink of the Kuroshio path off the Izu Peninsula on the Prompt Report edited on January 11, 2001 (upper left figure of Fig. 3). The kinked Kuroshio path can be seen from off Sagami Bay to Suruga Bay, and the warm water tongue extended westward from the tip of the kink passing off Ise Bay. We anticipated the generation of a new warm eddy, and sent the R/V Seisui-maru on January 12, 2001 to this area. The Prompt Report edited on January 18 (lower left figure of Fig. 3) indicated the formation of Eddy IV. The position of the observation XBT4 is shown on both of the Prompt Report figures (Fig.3). The temperature cross-section along the line is shown in the right figure of Fig. 3. The line runs through the central part of the warm eddy, and the temperature structure is monotonous except for Sta. XBT4-1, which was located at the edge of the warm eddy. It should be noted that the temperature at 200 m depth is between 17 and 18 ℃. The 15–16 ℃ isotherms at 200 m depth are used as indicators of the position of the current axis of the Kuroshio in the sea to the south of Japan. This high temperature indicates that the Kuroshio Water south of the axis had been brought into Warm Eddy IV.

The second observation (XBT5) of Warm Eddy IV was conducted on January 30. The position of the observation line is shown on the Prompt Report No. 5 edited on February 1, 2001 (left figure of Fig. 4), and the obtained temperature cross-section is shown in the right figure of Fig. 4. Though the observation line appears not to run across the central part of Warm Eddy IV, the temperature at 200 m depth exceeds 15 ℃ at all stations except at Sta. XBT5-1, indicating that the water near the current axis of the Kuroshio was kept inside of the warm eddy.

The third observation (XBT6) of Warm Eddy IV was conducted on March 5–6, 2001. The temperature cross-section is shown in the right figure of Fig. 5, and the observation line is shown in the left figure of Fig. 5 together with oceanic status on March 8. Sta. XBT6-7 appears to be located near to the center of Warm Eddy IV. The stations from Sta. XBT6-1 through Sta. XBT6-7 are aligned from west to east, and the

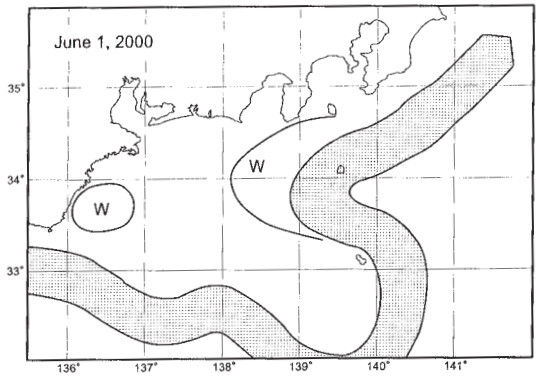

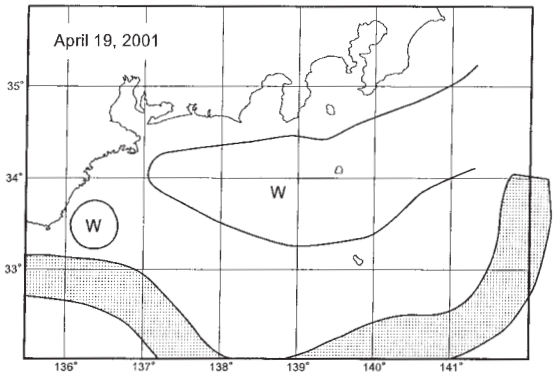

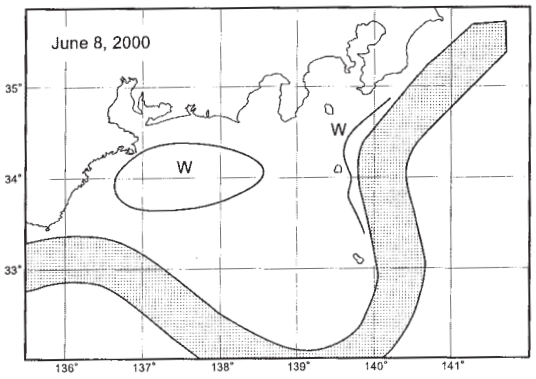

Fig. 8 The same as in Fig. 6 but for the reinforcement stage of Warm Eddy II on June 8, 2000.

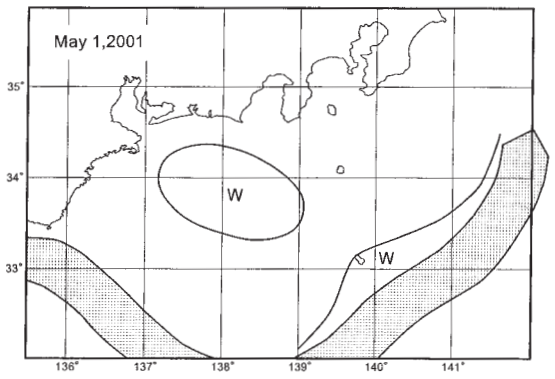

Fig. 9 The same as in Fig. 6 but for the reinforcement stage of Warm Eddy IV on May 1, 2001.

stations from Sta. XBT6-7 to Sta. XBT6-11 aligned from south to north. Judging from the temperature distribution, Sta. XBT6-1 and Sta. XBT6-11 were taken near the edge of Warm Eddy IV. The temperature at 200 m depth at Sta. XBT6-7 exceeds 17 ℃. Though the size of the eddy was significantly decreased by this time, the water at the center of the eddy maintained a high temperature corresponding to the current zone of the Kuroshio.

4-3. Thick structure of the stable warm eddies

As discussed above, both of the stable warm eddies had a thickness of several hundreds meters, and the temperature of the water inside the eddies was very high, and the water inside the eddies is thought to have originated from the Kuroshio current region. Thus, these eddies are sustainable for relatively long period. We shall discuss the generation procedure of these eddies by referring to the Prompt Reports in the next section.

5. Evolution of the oceanic status in the generation stage of the thick and stable warm eddies

The current zone of the Kuroshio is referred to from the Prompt Reports, and the evolution from the generation stage of Warm Eddy II is shown in Fig. 6. The current zone is shown as a hatched zone, and the relatively high temperature area inside the large meander of the Kuroshio is shown with bold lines. On February 24, a cold-water mass was seen to the southeast of the Kii Peninsula, and another cold-water mass to the southeast of the Boso Peninsula. The Kuroshio path shifted northward between the two cold-water masses, and a wide warm water region reached near to the coast. A kink of the Kuroshio path was seen off

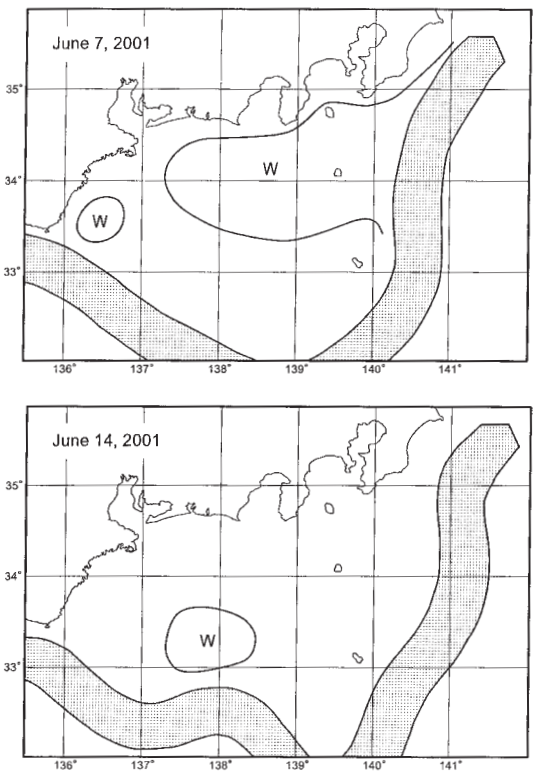

Fig. 10 The same as in Fig. 6 except for the reinforcement stage of Warm Eddy IV on June 14, 2001.

Cape Omaezaki (138° 10′ E), and warm water extended westward to off Ise Bay. A western cold-water mass developed, and its eastern margin shifted to the east from February 24 to March 9. While, the warm water tongue remained almost at the same position, and its east-west length increased gradually. Then, the main path of the Kuroshio retreated southward by March 16. The warm-water tongue widely extended in an east-west direction is seen from the tip of the retreated Kuroshio zone to off Kumano-nada on March 16. On March 23, an isolated warm eddy, Warm Eddy II, was generated off Enshu-nada from the warm-water tongue.

The evolution of the oceanic condition for the generation stage of Warm Eddy IV is shown in Fig. 7 in the same manner of Fig. 6. The Kuroshio path was kinked just off the Izu Peninsula on January 4, 2001 (upper figure), and a large warm-water tongue extending westwards was created on January 11 (middle figure). On January 18, an isolated warm eddy, Warm Eddy IV, was generated (lower figure). The sea level records at Hachijo and Miyake Islands indicated that the Kuroshio path had moved to the east of the Izu Ridge by January 18. The generation process of Warm Eddy IV is very similar to that of Warm Eddy II.

The temperature structure shown in the Prompt Report represents that for the surface layer. Judging from the vertical structure measured by XBT (the previous section), the Kuroshio Water appeared to intrude along the warm-water tongues much more than shown in Fig. 6 and Fig. 7. The origin of the warm water in the thick and stable warm eddies would be brought about by the cut off of the Kuroshio meander.

6. Reinforcement or replacement of thick and stable warm eddies

The thick and stable warm eddies were weakened several times: once on June 1, 2000 for Warm Eddy II and on April 19 and on June 7, 2001 for Warm Eddy IV as indicated in the last column in Table 1. The evolution of the oceanic conditions are shown in Fig. 8, Fig. 9 and Fig. 10, respectively. In each case, the warm eddy was weakened and moved near to the east of Cape Shionomisaki just before its reinforcement event (upper figures in Fig. 8, in Fig. 9 and in Fig. 10). At the same time, a warm-water tongue intruded from the east into the area under consideration. Then, one week later, the strengthened warm eddy was established off Enshu-nada.

The disappearance stage of the thick and stable warm eddies were not clear, but the weakened warm eddies shown in these upper figures resembles the situation of the disappearance stage. So, the reinforcement event shown here might be understood as the replacement of the old eddy by a newly generated warm eddy. If so, the period of continuation shown in Table 1 might be overestimated, but it is hard to conclude from the limited available data.

7. Sea level difference between Kushimoto and Uragami

The position of the Kuroshio axis off Cape Shionomisaki can be monitored by the sea level difference between Kushimoto and Uragami. KAWABE (1980) showed that the sea level difference (the sea level at Kushimoto minus that at Uragami) is small and is stable when the Kuroshio takes a typical meandering path and is large and very variable when the Kuroshio takes a straight path. FUJITA (1997) analyzed the correlation between the sea level difference between these two stations and the separation distance of the Kuroshio axis measured southward from the tip of the Kii Peninsula (Cape Shionomisaki) (see Fig. 11 of NAGATA *et al.*, 1999b) . When the Kuroshio takes a straight path and the distance is smaller than 50 km, the sea level difference is higher than 25 cm. While, when the Kuroshio takes a meandering path and the distance is larger than 50 km, the sea level difference is almost constant and less than 25 cm. (Here, the reported sea level values are used, and a 25 cm difference corresponds to a zero difference in absolute sea levels). FUJITA (1997) discussed about the half-month averaged values. TAKEUCHI *et al.* (1998) and NAGATA *et al.* (1999b) discussed the detailed oceanic structure in the vicinity of Cape Shionomisaki and clarified why the sea level difference is well correlated to the separation distance of the Kuroshio, and UCHIDA *et al.* (2000) indicated that the similar correlation is found even if daily averaged values are used.

However, a good correlation between the sea level difference and the separation distance of the Kuroshio could not be found in the period from January 2000 to May 2001 as shown in Fig. 11. The separation distance was very changeable, but the sea level difference was almost steady during this period. It is plausible that the appearance of the thick and stable warm eddies influenced the sea level at Uragami to minimize the sea level difference.

8. Concluding remarks

Two thick and stable warm eddies were found in 2000 and in 2001 inside the Kuroshio Large Meander. The period of continuation of these two warm eddies were 183 days and 218 days, respectively. These eddies were formed from warm-water tongues extending westward from the kinked current path of the Kuroshio off the Izn Peninsula, and contained the warm Kuroshio water up to several hundred meters in depth. The warm eddy reported by MINAMI (1989) would be very similar to these stable warm eddies, though its detailed nature was not fully clarified due to the limited observational data.

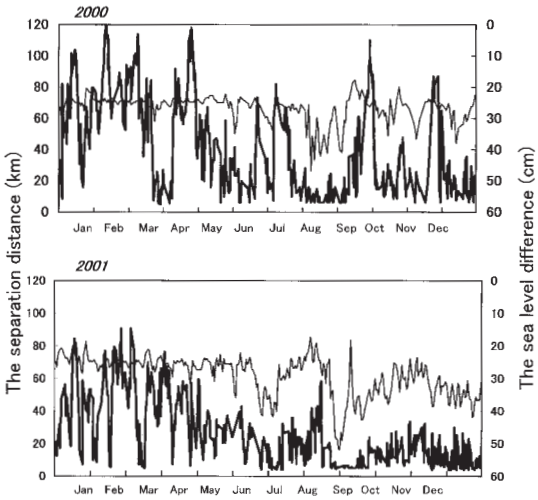

Fig. 11 Variations of the separation distance of the Kuroshio measured southward from the tip of the Kii Peninsula (Cape Shionomisaki) (bold line: the scale of distance is given on left side of the figure in km) and of the sea level difference between Kushimoto and Uragami (thin line: the scale is given on right side of the figure in cm) in the period from January 2000 to December 2001 (after J. Takeuchi of the Wakayama Research Center of Agriculture, Forestry, and Fisheries). Note that the scale of the sea level difference is given inversely.

Another warm eddy (Warm Eddy V) was formed on September 20, 2001 in a similar formation processes, but it had relatively short lifetime. The flow pattern of the Kuroshio was changed from the meandering path to straight path at the decaying stage of Warm Eddy V. If the warm eddy approaches to the current zone of the Kuroshio, strong current shear would be

generated and the warm eddy would become unstable. So, the stable warm eddy would be well separated by cold-water mass from the current zone of the Kuroshio. It is understandable that the stable warm eddy is usually from the warm-water tongue extended westward from off the Izu Peninsula, as the intruded warm water would be well separated from the current zone of the Kuroshio in such condition. Also, when the straight path is established, there would not be enough space to create a stable warm eddy off Enshu-nada.

Acknowledgements

We would like to thank Profs. Takashi KOIKE and Yoshitaka MORIKAWA of the Faculty of Bioresources for their valuable advice and discussions, and to the captain, Mr. Isamu ISHIKURA, and crew of R/V Seisui-maru for their help in the field observations. We also thank the staff of the MIRC Service Division, Ms. Keiko TAJIMA and Mr. Ken-ichiro SUZUKI of the Marine Information Center, JHA for their efforts to prepare the Prompt Report of Oceanic Status in the Sea off Sagami Bay and near the Izu Islands. Thanks are also due to Mr. Junichi TAKEUCHI of the Wakayama Research Center of Agriculture, Forestry and Fisheries, who supplied valuable research results to us.

References

FUJITA, K. (1997): Study on the relation between the variation of the Kuroshio path south of Japan and the sea level difference between Kushimoto and Uragami. Dr. Thesis, Faculty of Bioresources, Mie University 136 pp. (in Japanese)

FUJITA, K., Y. NAGATA and S. YOSHIDA (1998): Does small-scale meander travel eastwards and trigger large-scale meander of the Kuroshio. Acta Oceanographica Taiwanica, **37**, 127–138.

KASAI, A., S. KIMURA, and T. SUGIMOTO (1993): Warm water intrusion from the Kuroshio into the coastal areas south of Japan. J. Oceanogr., **49**, 607–624.

KAWABE, M.(1980): Sea level variation along the south coast of Japan and the large meander in the Kuroshio. J. Oceanogr. Soc. Japan, **36**, 227–235.

KIMURA, S. and T., SUGIMOTO (1990): Intrusion processes of warm mass from the Kuroshio into the coastal area of Kumano-nada and Enshu-nada Seas. Bull. Japan. Soc. Fish. Oceanogr., **54**, 19–31 (in Japanese) .

KOBAYASHI, M., T. SUGIMOTO, and T. HIRANO (1986): Surface current patterns in the Kumano-nada and the Enshu-nada Seas for different types of the Kuroshio paths based on GEK data– II, –For periods with large meander of the Kuroshio, Bull. Japan. Fish. Oceanogr., **50**, 2–11 (in Japanese).

MAEKAWA, Y., M. UCHIDA and Y. NAGATA (2001): Utilization of the near-real-time altimeter data given by Colorado Center for Astrodynamics Research of University of Colorado. Bull. Faculty of Bioresources, Mie University, **27**, 1–15 (in Japanese).

MINAMI, H. (1989): Warm water structure that approaches to Kii Peninsula, separated from the straight zonal Kuroshio path. La mer, **38**, 87–93 (in Japanese).

NAGATA, Y., S. YOSHIDA and K. FUJITA (1999a): Small scale meander as the trigger of the Kuroshio Large Meander. La mer, **36,** 119–130 (in Japanese).

NAGATA, Y., J. TAKEUCHI, M. UCHIDA, I. ISHIKURA, Y. MORIKAWA, and T. KOIKE (1999b): Current nature of the Kuroshio in the vicinity of the Kii Peninsula. J. Oceanogr., **55**, 407–416.

SEKINE, Y., and T. OKUBO (2000): Warm water structure that approaches to Kii Peninsula, separated from the straight zonal Kuroshio path. La mer, **39**, 87–93.

SHOJI, D. (1972): Time variation of the Kuroshio south of Japan. 217–234. In Kuroshio – Its Physical Aspect, H. STOMMEL and K. YOSHIDA, (eds.) Univ. of Tokyo Press.

TAFT, B. A. (1972): Characteristics of the flow of the Kuroshio south of Japan. 165–216. *In* Kuroshio – Its Physical Aspect, H. STOMMEL and K. YOSHIDA, (eds.) Univ. of Tokyo Press.

TAKEUCHI, J. (1989): Warm water intrusion in the southern area of Kumano-nada. Bull. Japan. Soc. Fish. Oceanogr., **53**, 242–254 (in Japanese).

TAKEUCHI, J., N. HONDA, Y. MORIKAWA, T. KOIKE and Y. NAGATA (1998): Bifurcation Current along the southwest coast of the Kii Peninsula. J. Oceanogr., **54**, 45–52.

UCHIDA, M., J. TAKEUCHI, Y. MORIKAWA, Y. MAEKAWA, O. MOMOSE, T. KOIKE and Y. NAGATA (2000): On structure and temporal variation of the Bifurcation Current off the Kii Peninsula. J. Oceanogr., **56**, 17–30.

Received October 11, 2002
Accepted November 14, 2002

La mer 40 : 183–189, 2002
Société franco-japonaise d'océanographie, Tokyo

画像解析によるヒラメ心拍数の計測

廣田　裕*，矢田　貞美*

Measurement of heart rate in *Paralichthys olivaceus* by image analysis

Yutaka HIROTA*, Sadami YADA*

Abstract : To count heart rates , we tried to analyze image of heartbeat movement which it permeated with the fiber light. In this paper, we used the juvenile flounder *Paralchthys olivaceus* in the case of normal and albinism fish body. The results are as follows.

1. In the same fish body width, a transmissivity of a fiber light of albinism fish was higher by 1.2 〜1.6 times than normal one.
2. There was need 10,030 lx for analyzing the fish body width 6.85 mm. When a fish body width was widened, a minimum illuminance to permeate the heart increased.
3. The high correlation was recognized between operculum moving number and heart rate in condition of optical irradiation.
4. The preparation time to measure the heart rate with this system needs for approximately 40 minutes.

This measuring method is useful to research the physiological influence of fish body in the external environment changing and the anesthesia treatment.

Keywords : *heart rate, operculum moving number, Paralchthys olivaceus , image analysis*

1. はじめに

魚類の心電図を計測する方法には，まず電極を囲心腔に埋め込む体内導出法（OITS *et al.*, 1957; NOSEDA *et al.,* 1963; NOMURA *et al.*, 1969; 難波ら,1973; 難波, 1978, 1996）があげられる。体内導出法は，麻酔処理した魚の心臓部をリード線と一体となった一対の電極で挟持して心電図を計測する。心筋の起電力が小さいコイ科の魚類や遊泳魚体でも波形解析が可能であるが，麻酔処理および体内への電極挿入が安静状態の心拍数に影響を及ぼすことが危惧される。次に，電極を魚体表面に設置する体表面導出法（OETS, 1950; 山森ら，1971a; 伊東, 1998）があげられる。心臓の起電力が大きいウナギでは，水中の魚体表面近傍に電極を設置することでも心電図の計測が可能である（山森ら，1971b)。体表面導出法は固定した供試魚の鰓に麻酔液を環流し，体表面における電極設置部位別の心電図を長時間計測することが可能であるが，やはり麻酔処理が必要である。そこで，非接触かつ非麻酔処理で遊泳魚の体表面より微弱電流を取り出す計測方法（野村・秋山, 1984）が開発された。この方法は魚体を損傷させないが，遊泳魚の心電図計測では，電極近傍に魚体をとどめるために適当な水流条件下において前進遊泳を停止させる（以降，滞泳と称する)。そのため，魚体の大小および魚種により流速を変化させる必要があり，一定の運動量下における計測は困難である。

一方，光照射が魚類に与える影響については，魚類の行動および生理の分野において研究されてきた。魚類は，低照度下においては光源に蝟集するが，高照度下においては光源から逃避する（今村, 1968)。魚類生理学の分野では，光に対する魚の網膜反応の程度を判定する際に，心電図や心拍数を利用した研究が多く行われている。これらの研究には，コントラスト（HESTER, 1968; ANTHONY, 1981)，偏光（KAWAMURA *et al.*, 1981; HAWRYSHYN and MCFARLAND, 1987)，紫外線（HAWRYSHYN and BEAUCHAMP, 1985)，レーザ光（川村ら，1991）およびストロボ光（安・有元, 1994）を10

* 東京水産大学海洋生産学科
〒108–8477　東京都港区港南4–5–7
Department of Marine Science and Technology, Tokyo University of Fisheries, 4–5–7 Konan, Minato, Tokyo, 108–8477 Japan

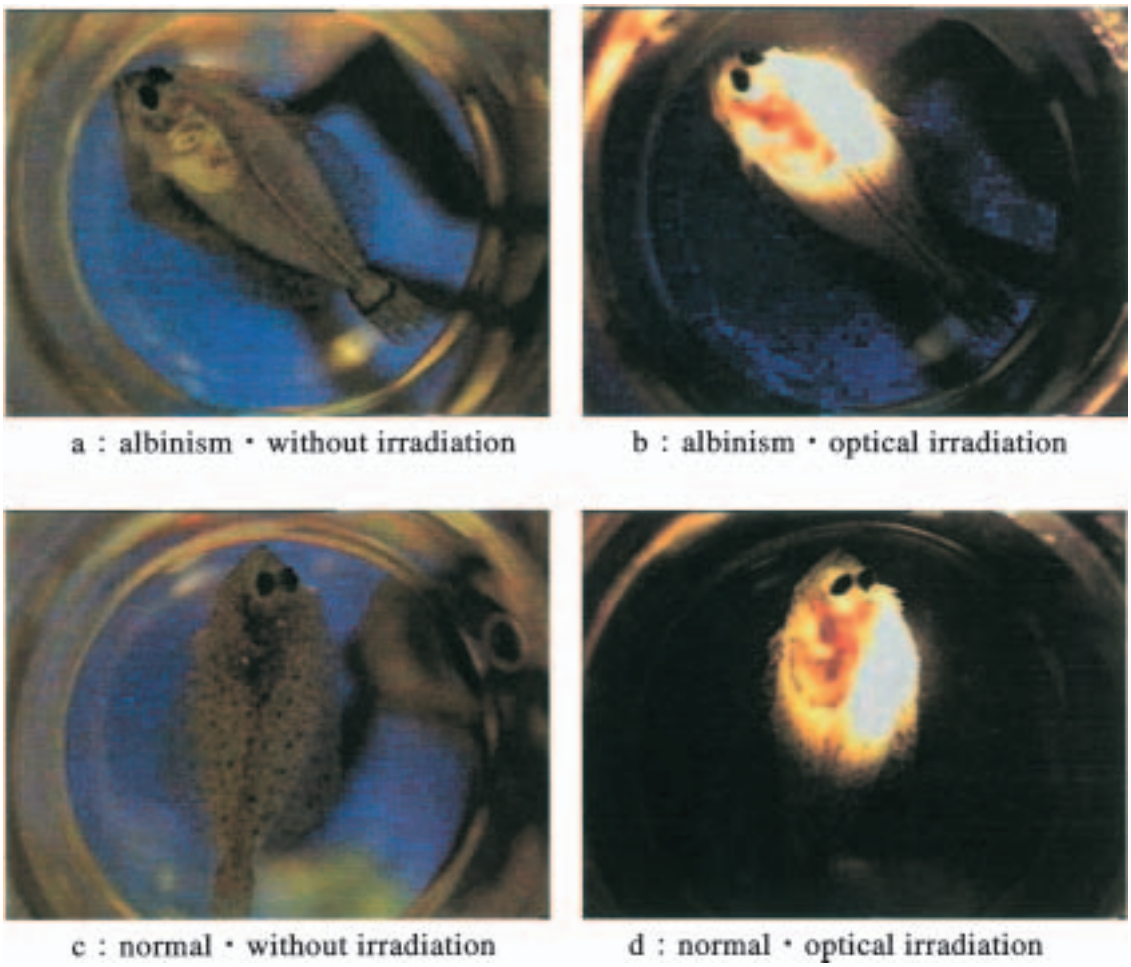

Fig. 1. Photography image of *Paralchthys olivaceus*
a : albinism • without irradiation. b : albinism • optical irradiation. c : normal • without irradiation. d : normal • optical irradiation.
a : Heartbeat movement can observe from back of fish body without irradiation. b : Heartb eat movement can observe under the low iluminance. c : Heartbeat movement can't observe without irradiation. d : Heartbeat movement can observe under the high iluminance.

Table 1 Size of test *Paralchthys olivaceus*

	Albinism Mean S.D.	Normal Mean S.D.
Body length (㎜)	26.21±1.27	56.65±8.00
Body width (㎜)	2.75±0.08	4.64±0.55
Body weight (g)	0.41±0.05	3.03±0.82
n	10	10
Relationship BL vs BW	y=0.06x+1.1, r=0.99	y=0.06x+0.82, r=0.99

秒以内の短時間光照射したものや白熱灯（安, 1996）を連続照射したものが含まれる。しかし，心拍数の計測を目的とした光利用に関する報告は見あたらない。既往の心拍数計測方法では，麻酔処理および体内への電極挿入が心拍数に影響を及ぼす短所があった。

そこで本報では，一般に心臓の鼓動数と心拍数は同数であるので，光照射による心臓部の撮影画像の解析，すなわち心臓の鼓動数を心拍数として計測する方法の確立を目的とした。また，供試魚を計測用容器に移し換える行為ならびに光照射照度の高低が心拍数に及ぼす影響を定量的に捉え，安静時における心拍数の計測について検討した。

なお，本研究は，色素が薄いため室内レベルの照度でも魚体裏面より心臓の鼓動が目視可能な白化個体の特徴に着目したものである。白化現象は，人工採苗した稚魚に多く見られ，その原因解明および防除のための研究が行われている（京都府海洋センター，1983; 福所ら，1986; 竹内, 1998）。

2. 方　法

1）供試魚

ヒラメ*Paralchthys olivaceus*の幼魚を供試した。正常個体および体色異常の白化個体各10尾を水温20±1.0℃の透明アクリル製水槽（縦30cm×横59cm×高さ34cm）で蓄養した。

Table 1にヒラメのサイズを，Fig. 1にヒラメの撮影画像をそれぞれ示す。正常個体および白化個体の体長と体幅との間には正の相関が認められた。白化個体では，約250 lxの照度下で目視による心拍数の計数が可能であった。

2）計測装置

Fig. 2に計測システムの概略図を示す。同システムは主に，光源，ガラス水槽，計測用容器，ビデオカメラ，ディスプレイおよび濾過装置で構成される。光源には魚体および水槽内の海水に熱影響を与えない高輝度冷光装置（林時計(株)製，150 W）を使用した。同冷光装置および発光部を接続するファイバープローブの先端径は5㎜であり，被接写体位置の照度を1,400〜16,000 lxまで無段階に調整可能である。供試体の遊泳範囲を制限するため，主実験領域であるガラス水槽（縦19cm×横29cm×高さ20cm）内に，さらに透明アクリル製の計測用容器（縦10cm×横10cm×高さ10cm）を設置した。ガラス水槽および計測用容器の水深は3.5cmに設定し，人工海水（千寿製薬社製，Marine art SF）を使用した。水質保持を目的として，実験中は散気および濾過装置を稼動させ，蓄養水槽と同様に水温を20±1.0℃に制御した。

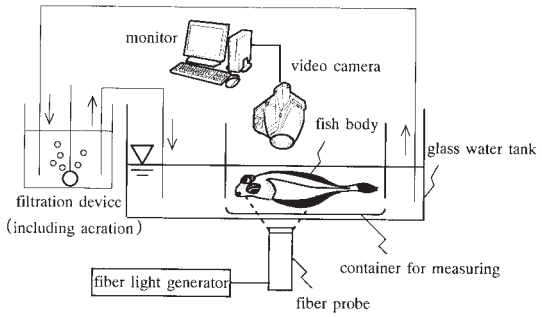

Fig. 2. System for measuring heart rate.

3）計測方法

（1）概要

計測容器内における魚体の心臓部を冷光照射し，撮影画像の解析により鰓蓋開閉数および心拍数を計測する方法の概要を以下に述べる。まず，蓄養水槽からガラス水槽内の計測用容器へ魚体を移し換える（以降，水槽移換と称する）。水槽移換から平常状態，すなわち鰓蓋開閉数および心拍数が安静時の値まで回復（以降，安静化と称する）した魚体の心臓部に冷光を照射して透過する。次に，魚体の鰓蓋および心臓部の画像をビデオカメラで撮影し，その記録画像から毎分の鰓蓋開閉数および心拍数を計数する。

ここで事前に，ヒラメの心臓部の光透過特性と，供試魚が水槽移換および光照射直後から安静状態に達するまでの時間（以降，安静化所要時間と称する）とを把握しておく必要が生じる。心臓部の光透過特性に関しては，まず一定照度の冷光を照射して光透過率を求めた。次に，徐々に照度を上昇させて光透過限界照度を求めた。安静化所要時間に関しては，まず自然飼育，すなわち魚体に刺激を与えない状態の鰓蓋開閉数および心拍数を計数し，これを安静時の各値と定義した。次に，撮影画像より魚体の水槽移換および光照射後の鰓蓋開閉数および心拍数を計数して，安静化所要時間を求めた。

なお，安静時および水槽移換後の心拍数の計測には，魚体裏面から鼓動が観察可能な白化個体のみを供試した。

（2）心臓部の光透過特性

供試魚を1尾ずつ計測用容器内に入れ，冷光の照度を2,000 lxに設定し，魚体下方1cmから心臓部に対して垂直上向きに照射した。光軸上の透過光の照度を魚体上方10cmに設置した照度計（東京硝子器械(株)製，FLX-1334）により計測し，心臓部の光透過率（%）を次式(1)より求めた。

$$T_s = \frac{L_\beta}{L_\alpha} \times 100 \qquad (1)$$

ただし，T_s：心臓部の光透過率（%），L_α：照射光の照度（lx），L_β：心臓部の透過照度（lx）である。

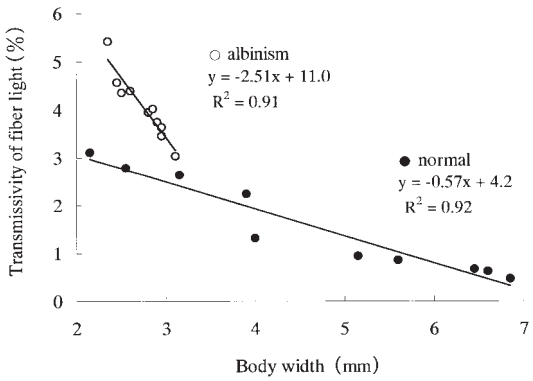

Fig. 3. Relationship between transmissivity of a fiber light and body width.

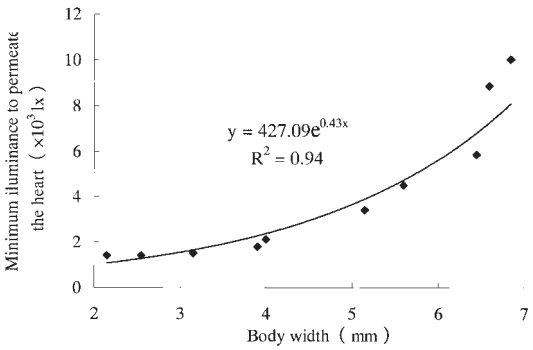

Fig. 4. Relationship between minimum iluminance to permeate the heart and body width.

さらに，体幅と心臓部の透過限界照度との関係を求めた。供試魚を1尾ずつ計測用容器内に入れ，冷光を魚体下方1cmから心臓部対して垂直上向きに照射し，光源の照度を設定下限である1,400 lxから徐々に上昇させる。魚体上方10cmから垂直下向きに撮影した心臓部の画像をディスプレイ上で観察し，鼓動が観察可能となる下限照度を心臓部の光透過限界照度とした。

（3）安静時の鰓蓋開閉数および心拍数の計測

鰓蓋開閉数の計測には正常個体および白化個体を供試し，飼育水槽内における鰓蓋開閉数を目視で計数した。10分間の鰓蓋の開閉数より，毎分の平均鰓蓋開閉数を算出した。心拍数の計測には白化個体のみを供試し，計測用容器へ水槽移換60分後から10分間魚体を撮影した。ビデオカメラを魚体下方10cmに設置し，垂直上向きに撮影した画像より，毎分の平均心拍数を算出した。

（4）水槽移換後の鰓蓋開閉数および心拍数の計測

飼育水槽から計測用容器内へ魚体を水槽移換した直後から60分間，魚体を撮影した。鰓蓋開閉数の計測には正常個体および白化個体を供試し，ビデオカメラを魚体上方10cmに設置して，垂直下向きに撮影した。心拍数の計測には白化個体のみを供試し，ビデオカメラを魚体下方10cmに設置し，垂直上向きに撮影した。撮影画像より，毎分の平均鰓蓋開閉数および心拍数を算出し，安静化所要時間を求めた。

（5）光照射後の鰓蓋開閉数および心拍数の計測

計測用容器内で安静化した正常個体および白化個体の心臓部に冷光を照射し，照射直後から60分間，魚体を撮影した。光源を魚体下方1cmに設置し，垂直上向きに照射した。心臓部の光透過限界照度の測定結果より，照度は1,800 lx（以降，低照度と称する）および10,030 lx（以降，高照度と称する）の2段階に設定した。なお，低照度では大型の正常個体の心臓部は光透過できないので，体幅が3.5㎜以下の魚体のみを供試した。ビデオカメラを光軸の延長線上に設置し，魚体上方10cmから垂直下向きに撮影した。撮影画像より，毎分の平均鰓蓋開閉数および心拍数を算出し，安静化所要時間を求めた。

3. 結　果

1）心臓部の光透過特性

Fig. 3に正常個体および白化個体の体幅と心臓部の光透過率との関係を示す。光透過率は，体幅が大きいほど減少し，同体幅の場合，白化個体の方が正常個体より1.2〜1.6倍高かった。Fig. 4に正常個体の体幅と心臓部の光透過限界照度との関係を示す。体幅が大きいほど光透過限界照度は増加し，体幅2.55㎜以下では1,400 lxで鼓動が観察できたが，体幅6.85㎜では10,030 lxを要した。白化個体は体幅の大小にかかわらず，1,400 lxで鼓動が観察できた。

2）安静時の鰓蓋開閉数および心拍数

Table 2に安静時の鰓蓋開閉数および心拍数を示す。正常個体および白化個体の毎分の平均鰓蓋開閉数はほぼ同程度であった。白化個体の毎分の平均心拍数は約88回であった。

3）水槽移換後の鰓蓋開閉数および心拍数

Fig. 5に水槽移換直後から30分間の鰓蓋開閉数および心拍数を5分間隔で示す。水槽移換直後の鰓蓋開閉数は安静時の1.5〜1.7倍に，心拍数は安静時の1.4〜1.5倍に増加した。鰓蓋開閉数および心拍数の安静化所要時間は10分程度であった。なお，水槽移換に要した時間は約3秒であった。

4）光照射後の鰓蓋開閉数および心拍数

Fig. 6に低照度光照射直後から30分間の鰓蓋開閉数および心拍数を5分間隔で示す。光照射直後の鰓蓋開閉数は白化の有無にかかわらず，安静時の約1.2倍増加した。

Table 2 Operculum moving number and heart rate when a fish body is normal condition.

	Albinism Mean S.D.	Normal MeanS.D.
Operculum moving number (times/min)	54.2±1.25	54.3±1.01
Heart rate (times/min)	87.8±1.97	−
n	10	10

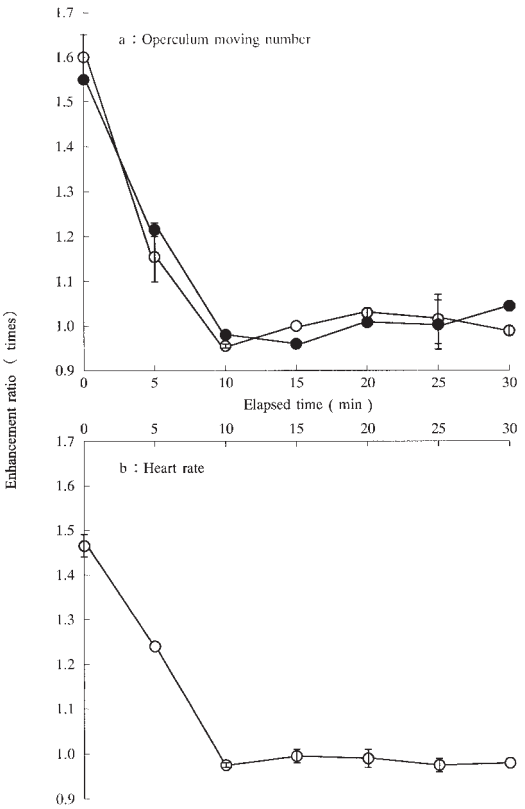

Fig. 5. The enhancement ratio of operculum moving number and heart rate when a fish body was transfered into other water tank. ●：normal. ○：albinism.

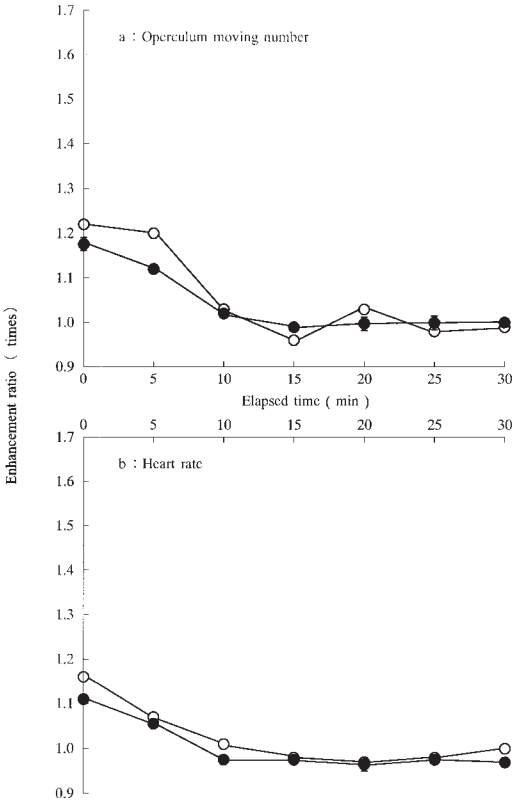

Fig. 6. The enhancement ratio of operculum moving number and heart rate under the low iluminance. ●：normal. ○：albinism.

一方，心拍数は，正常個体で安静時の約1.1倍に，白化個体で安静時の約1.2倍に増加した。鰓蓋開閉数および心拍数の安静化所要時間は，15分程度であった。

Fig. 7に高照度光照射直後から30分間の鰓蓋開閉数および心拍数を5分間隔で示す。光照射直後の鰓蓋開閉数は，正常個体で安静時の約1.2倍に，白化個体で安静時の約1.3倍に増加した。一方，心拍数は，白化の有無にかかわらず，安静時の約1.2倍に増加した。鰓蓋開閉数および心拍数の安静化所要時間は，25〜30分程度であった。

5）鰓蓋開閉数と心拍数との関係

水槽移換後，光照射後に同一個体から同時に得られた，鰓蓋開閉数と心拍数との関係をFig. 8に示す。白化の有無にかかわらず，鰓蓋開閉数と心拍数との間には高い正の相関が認められた（正常個体：r＝0.96，白化個体：r＝0.92）。

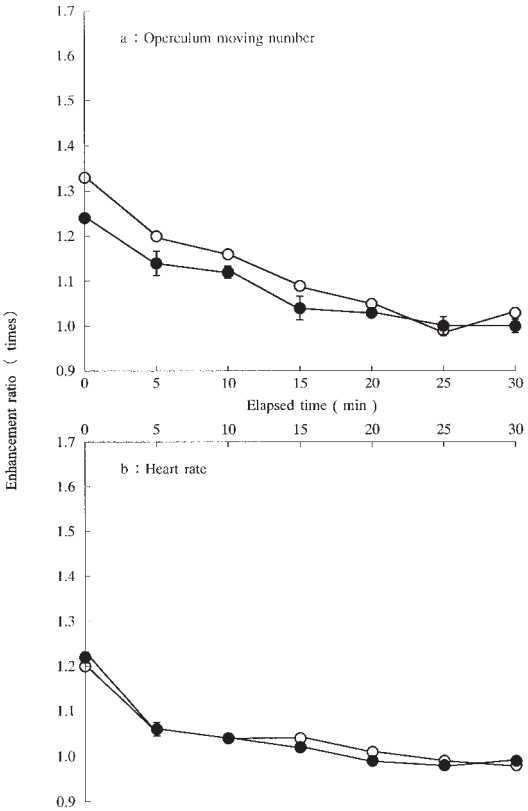

Fig. 7. The enhancement ratio of operculum moving number and heart rate under the high iluminance. ●：normal. ○：albinism.

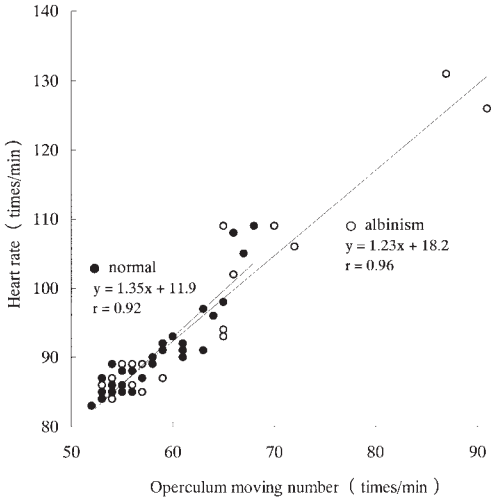

Fig. 8. Relationship between operculum moving number and heart rate.

4. 考　察

鰓蓋開閉数と心拍数との間には，高い正の相関が認められた（Fig. 8）。このことより，鰓蓋開閉数は心拍数を示す指標となり得るものと考えられる。水槽移換後には，正常個体および白化個体の鰓蓋開閉数に差は認められず（Fig. 5），また白化個体の鰓蓋開閉数と心拍数との間には正の相関が認められることから，正常個体の心拍数の安静化所要時間も，白化個体と同様に10分程度であると推定される。

光照射直後の正常個体および白化個体の心拍数は，安静時と比べて1.1〜1.3倍に増加した（Fig. 6，7）。白熱灯を照射したコイの心拍数は，水中における照度が300 lx下では照射前とほとんど変化がなく，700 lx下では照射前の約1.5倍に，1,400 lx下では照射前の3〜4倍に増加する（安，1996）。本報とは魚体への光照射の目的および方法は異なるが，いずれも光照射による心拍数の増加を回避することはできない。

光照射直後の鰓蓋開閉数および心拍数の増加率は，高照度光照射直後の心拍数を除いて，白化個体の方が正常個体より高い傾向が見られた。この原因としては，心臓部の光透過率が白化個体の方が正常個体より高く（Fig. 3），より多くの光刺激を視覚に受けたためと考えられる。

安静化所要時間は，水槽移換後で10分程度，低照度光照射後で15分程度，高照度光照射後で30分程度であった。これらを合計すると，本システムにより心拍数を計数するための準備時間は最長で40分程度を要するが，水槽移換と光照射を行うことで，水槽移換の影響を光照射の影響に抱合させることができ，安静化所要時間を短縮できるものと推定される。光照射後の安静化所要時間の方が，水槽移換後の安静化所要時間より長かったことから，ヒラメは接触刺激よりも，光刺激に対する環境順応に長時間を要するものと考えられる。

本方法の特徴は，魚体に非接触かつ非麻酔処理で心拍数を計測することにあるが，魚体への光照射を回避することはできない。実験中に供試魚が発光部から逃避することはほとんど認められなかったが，これはヒラメの低移動性，ならびに同魚の両眼が光照射方向と反対の魚体表面に位置することによるものと思われる。それゆえに，カレイなど移動性が低く体幅の小さい魚類，ならびに魚体色素の薄いトランスルーセントキャットフィッシュ，カワエビなどの心拍数の計測には有用と思われる。移動性の高い魚種へ適用する場合，魚体サイズに適合した容器，もしくは適当な水流条件が設定可能な水槽を準備し，滞泳する魚体の心臓部と光源が同軸上になるように設定する必要がある。

今後，プローブ先端径の大小，同プローブと被接写体間の距離，ならびに光源の出力を変化させることにより，画像撮影位置における照度をより細かく調整することが

可能となる。本方法では，同一の撮影画像から鰓蓋開閉数および心拍数を計数するために，ヒラメのサイズならびに鰓蓋と心臓間の距離を考慮し，先端径5㎜のプローブを使用した。心拍数のみを計数する場合，プローブ先端径を小さくすることで，供試魚の視覚に対してより低刺激の状態で計数が可能になるものと考えられる。現行装置の照度の設定下限は1,400 lxであるが，プローブと被接写体間の距離を長くとることで照射スポット径は拡大し，1,400 lx以下の調光が可能となる。光透過率の高い魚種，ならびに体幅の小さい魚体には，より低照度かつ低刺激で計数が可能となる。これに対して，強力な光源を用いることで，照度を現行装置の設定上限である16,000 lx以上に設定できると，光透過率の低い魚種，ならびに体幅の大きい魚体にも心臓部の光透過が可能になると期待される。

本方法では，魚体裏面から光を照射しているため，魚体表面に魚眼を持つヒラメは魚体を透過した照度を体感していると考えられる。本方法を利用して，ストロボ光やレーザ光などの各種刺激光に対する網膜反応の程度を判定する際には，心臓部への照射光が魚眼への刺激光に重複されることを考慮に入れる必要がある。その一方で本方法は，例えば計測用容器内の水質および水温などの環境変化，ならびに麻酔処理が鰓蓋開閉数および心拍数に及ぼす生理的影響を明らかにするには好適と思われる。

残された課題としては，より刺激の少ない光波長域の探索があげられる。

謝　辞

査読者には懇切丁寧なご指導を頂きました。ここに，深く感謝申し上げます。

文　献

安永一・有元貴文（1994）：ストロボ光に対するマアジの回避行動．日本水産学会誌，**60**，713–718.

安永一（1996）：心電図による光刺激効果の判定．魚の行動生理学と漁法（日本水産学会編），恒星社厚生閣，東京，**108**，86–95.

Anthony, P.D.（1981）: Visual contrast thresholds in the *Cod Gadus morhua* L.J. Fish Biol., **19**, 87–103.

福所邦彦・山本剛史・青梅忠久（1986）：ヒラメの白化体出現におよぼす飼育中の通気量の影響．Bull. Nati. Res. Inst. Aquaculture., **10**, 53–56.

Hawryshyn, C.W. and R. Beauchamp（1985）: Ultraviolet photosensitivity in goldfish; An independent U.V. reninal mechanism. Vision Res., **25**, 11–20.

Hawryshyn, C.W. and W.N. McFarland（1987）: Cone photorecepter mechanisms and the detection of polarized light in fish. J. Comp. Physiol. A., **160,** 459–465.

Hester, F.J.（1968）: Visual contrast thresholds of the goldfish. Vision Res., **8**, 1315–1335.

今村豊（1968）：漁業における火光の集魚効果とその操法の研究（Ⅰ）．うみ，**6**，17–43.

伊東裕子（1998）：心電図測定による魚類の運動特性の解析に関する研究．東京水産大学大学院水産学研究科，修士論文，79pp.

Kawamura, G., A. Shibata and T. Yonemori（1981）: Response of teleosts to the plane of polarized light as determined by the heart rate. Bull. Japan. Soc. Sci. Fish., **47**, 727–729.

川村軍群・法花正志・荒牧孝行・新村厳（1991）：マダイによるHeNレーザー光線視認．日本水産学会誌，**57**，421–424.

京都府海洋センター（1983）：人口採苗ヒラメの体色異常の発生機構と防除に関する研究．昭和57年度京都府海洋センター事業概要，27–28.

難波憲二・村地四郎・河本真二・中野義久（1973）：魚類の心電図に関する研究―Ⅰ．心電図の導出方法の検討，広島大学水産学部紀要，**12**，147–154.

難波憲二（1978）：魚類心電図の導出方法．魚の呼吸と循環（日本水産学会編），恒星社厚生閣，東京，**24**，129–131.

難波憲二（1996）：魚類の心電図．魚の行動生理学と漁法（日本水産学会編），恒星社厚生閣，東京，**108**，74–85.

野村和夫・秋山勲（1984）：自由遊泳時の心電図測定方法の考案．日本水産学会誌，**50**，959–967.

Nomura, S., T. Ibaraki and S. Shirahata（1969）: Electrocardiogram of the rainbow trout and its radio transmission. Jap. J. vet. sci., **31**, 135–137.

Noseda, V., F. CHIESA and R. Marchetti（1963）: Vectorcardiogram of *Anguilla angilla* L. and *Pleurodeles waltlii* Mich. Nature, **197**, 816–818.

Oets, J.（1950）: Electrocardiograms of fishes. Physiol. Comp. et Oecolg., **2**, 181–186.

Oits, L.S., J.A. Cerf and G.J. Thomas（1957）: Conditioned inhibition of respiration and heart rate in the goldfish. Science, **126**, 263–264.

竹内俊郎（1998）：ヒラメ仔稚魚の栄養要求．平成10年度栽培漁業技術研修事業基礎理論コース，仔稚魚期の発育シリーズ，**11**，11–16.

山森邦夫・羽生功・日比谷京（1971a）：ウナギ体表心電図の単極導出法．日本水産学会誌，**37**，90–93.

山森邦夫・羽生功・日比谷京（1971b）：ウナギ心電図の水中電極による導出．日本水産学会誌，**37**，94–97.

2002年7月7日受付
2002年12月2日受理

La mer 40 : 191–202, 2002
Société franco-japonaise d'océanographie, Tokyo

On the Possibility of Improving the Flow and Water Quality in a Closed Inland Bay by Using Cooling Water for a Power Generating Plant

Tairyu TAKANO*, Michihiro SHIBAZAKI** and Akira WADA***

Abstract : A quasi 3-dimensional flow model and a water quality model (the Chesapeake Bay Model) were applied to a hypothetical power station to investigate whether it is possible that the intake and discharge of cooling water for a station located on a closed inland bay might bring beneficial change to the oceanic environment. The results of the flow and water quality calculations show that the intake and discharge of cooling water promote water exchange in the inland bay; in particular, there is accelerated exchange of the nutrient - enriched water inside the bay with cleaner water from outside the bay, so that there is at least a possibility that water quality will gradually be improved. In addition, bottom water pumped up continuously in front of the power plant brings about water quality changes in a concentric circular pattern: significant water quality changes are limited to the region within which the sea water temperature rises 1℃ or more.

Keywords : *Water flow and water quality analysis. Cooling water discharge*

1. Introduction

In Japan there are many thermal and atomic power plants, which are located along the coast so that they can use seawater for cooling. These power plants do not release pollutants into the water, but by affecting the water flow and temperature fields, they must have secondary effects on the marine environment. Until now most investigations on the environmental effect of the power plant discharges have been limited to investigating the extent of the area within which water temperature increases. But recent progress in methods of modeling water quality has made it possible to investigate the change of water quality as well.

When warm water is discharged from a power plant, the water temperature in the ocean in front of the power plant rises, causing photosynthesis to become more active and phytoplankton to multiply. If the water is rich in nutrients, this can give rise to more water pollution. However, at the same time intake and discharge of cooling water by the power plant promotes greater circulation of the water in the bay, which can be expected to have the effect of transporting nutrients out of the bay, (SUDO, 1993) so it is unclear what net effect there will be if the power plant is located at the shore of a closed inland bay. For this reason, we have performed calculations with a flow and water quality model to estimate the difference that can be expected between the present situation in such a bay and the situation that would exist if a power plant were built on its shore. There was particular interest in the possibility that the cooling water discharge might enhance the water flow and improve the water quality. We took as the object of our study Mikawa Bay (Fig. 1), where at present there is no power plant in the interior of the bay, in the summertime, when water quality is known to deteriorate.

* Laboratory of Aquatic Science Consultant Corporation, Kami Ikedai 1-14-1, Ota-ku, Tokyo, 145-0064, Japan
** Marine Ecology Research Institute, Kanda Jimbo-Cho 3-29 Chiyoda-ku, Tokyo, 101-0051, Japan
*** College of Industrial Technology, Nihon University, Izumi 1-2-1, Narashino, Chiba, 275-8575, Japan.

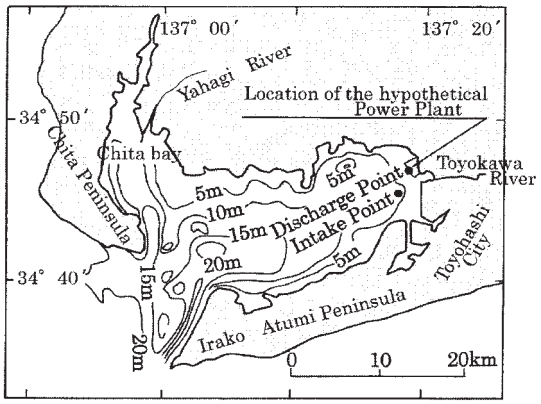

Fig. 1. Bottom topography of Mikawa Bay and the location of the hypothetical power plant.

2. The Model Calculation Method

2.1 The basic equations of the flow model

The tides in Mikawa Bay have strong cooscillating tide characteristics. The long axis of the M_2 tide is along the long axis of the bay; proceeding along this axis toward the interior of the bay, its amplitude decreases to 1/10 of its value at the mouth (UNOKI, 1978). The mean current, which consists of a component caused by the river inflow and the tidal residual current, primarily controls the transport of matter. In the flow calculation, the tide, density structure, river inflow and heat exchange at the sea surface are considered. The model consists of momentum, continuity and heat and salt diffusion equations.

• Equations of conservation of momentum

$$\frac{\partial u}{\partial t}+u\frac{\partial u}{\partial x}+v\frac{\partial u}{\partial y}+w\frac{\partial u}{\partial z}-fv = -\frac{1}{\rho}\frac{\partial P}{\partial x}+A_x\frac{\partial^2 u}{\partial x^2}+A_y\frac{\partial^2 u}{\partial y^2}+A_z\frac{\partial^2 u}{\partial z^2}, \quad (1)$$

$$\frac{\partial v}{\partial t}+u\frac{\partial v}{\partial x}+v\frac{\partial v}{\partial y}+w\frac{\partial v}{\partial z}+fu = -\frac{1}{\rho}\frac{\partial P}{\partial y}+A_x\frac{\partial^2 v}{\partial x^2}+A_y\frac{\partial^2 v}{\partial y^2}+A_z\frac{\partial^2 v}{\partial z^2}. \quad (2)$$

• Continuity equation

$$\frac{\partial u}{\partial x}+\frac{\partial v}{\partial y}+\frac{\partial w}{\partial z}=0. \quad (3)$$

• Surface boundary condition

$$\frac{\partial \zeta}{\partial t}+\left(u_s\frac{\partial \zeta}{\partial x}+v_s\frac{\partial \zeta}{\partial y}+w_s\right)_{z=\zeta_0}=0. \quad (4)$$

• Hydrostatic equation and equation of state

$$P_z=g\int_z^{\zeta}\rho dz, \quad (5)$$

$$\rho=\rho_S(T,\ S). \quad (6)$$

• Heat diffusion equation

$$\frac{\partial T}{\partial t}+u\frac{\partial T}{\partial x}+v\frac{\partial T}{\partial y}+w\frac{\partial T}{\partial z}= \frac{\partial}{\partial x}\left(K_x\frac{\partial T}{\partial x}\right)+\frac{\partial}{\partial y}\left(K_y\frac{\partial T}{\partial y}\right)+\frac{\partial}{\partial z}\left(K_z\frac{\partial T}{\partial z}\right)+\frac{1}{C\cdot\rho}\frac{\partial}{\partial z}(Q_1-Q_0). \quad (7)$$

• Salt diffusion equation

$$\frac{\partial S}{\partial t}+u\frac{\partial S}{\partial x}+v\frac{\partial S}{\partial y}+w\frac{\partial S}{\partial z}=\frac{\partial}{\partial x}\left(K_x\frac{\partial S}{\partial x}\right)+\frac{\partial}{\partial y}\left(K_y\frac{\partial S}{\partial y}\right)+\frac{\partial}{\partial z}\left(K_z\frac{\partial S}{\partial z}\right). \quad (8)$$

Here, t is time; x, y and z are the space coordinates; u, v and w are the velocity components in the x, y and z directions, respectively; u_s, v_s and w_s are the velocity components at the sea surface; A_x, A_y and A_z are the eddy viscosity coefficients in the coordinate directions; ζ is water level; P is pressure; g is gravitational acceleration; ρ is density; ρ_S is a reference density; C is specific heat; T is water temperature; S is salinity; K_x, K_y and K_z are the eddy diffusion coefficients in the coordinate directions; Q_1 is the flux of heat exchange with the atmosphere; Q_0 is the flux of heat exchange with the atmosphere at the initial water temperature, at grid points not on the sea surface $Q_1=Q_0=0$.

Q_1 and Q_0 are shown by the following equations

$$Q_1, Q_0=Q_s-(Q_b+Q_c+Q_e),$$
$$Q_s=0.239(1-\alpha)\beta Q_{s0}$$
$$Q_b=0.315\times10^{-12}(273+T)^4-0.296\times10^{-17}(273+T_a)^6(1+0.17C_d^2)$$
$$Q_c=0.0069C_H(T-T_a)u10$$
$$Q_e=0.010C_E(e_w-e_a)u10.$$

Here Q_s is the absorptive solar radiation; Q_{s0} is the solar radiation; Q_b is the effective long wave radiation; Q_c is the sensible heat flux; Q_e is the latent heat flux; α is the heat reflection coefficient of sea surface (0.060 in August); β is the heat absorption coefficient of sea surface (0.69); T is the water temperature, T_a is the air temperature, C_d is Cloud amount (0〜1); C_H is the sensible heat transport coefficient; C_E is the latent heat transport coefficient; u_{10} is the wind speed in 10m above sea surface; e_w is the saturated water vapor pressure at T and e_a is the water vapor pressure in the atmosphere.

2.2 Boundary conditions of the flow model

At the sea surface, $\partial u/\partial z=\partial v/\partial z=0$ and $\partial T/\partial z=\partial S/\partial z=0$. At the bottom, $u=v=0$ and $\partial T/\partial z=\partial S/\partial z=0$. Heat exchange with the atmosphere is treated as an external force. At the boundary with land, $u=v=0$ and $\partial T/\partial l=\partial S/\partial l=0$. Here l is vertical direction toward boundary. The tide at the open boundary is assumed to be the M_2 tide of a period of 12 hours with a sinusoidal curve. The flow is assumed to have zero first derivatives at normal to the boundary. Water temperature and salinity at this boundary are adjusted to the values of the open ocean when there is inflow; when there is outflow, the second derivative is assumed to be zero.

2.3 Basic equations of the water quality model

The water quality model consists of equations for the advection and diffusion of water quality elements (MULLIGAN, 1987). Letting C be the present value of one of the water quality elements, the equation for the local change with C over time is expressed in terms of advection, diffusion, inflow load, settling, deposition and biochemical processes by the following equation.

$$\frac{\partial C}{\partial t}=\frac{\partial}{\partial x}\left(K_x\frac{\partial C}{\partial x}\right)+\frac{\partial}{\partial y}\left(K_y\frac{\partial C}{\partial y}\right)+\frac{\partial}{\partial z}\left(K_z\frac{\partial C}{\partial z}\right)-u\frac{\partial C}{\partial x}-v\frac{\partial C}{\partial y}-w\frac{\partial C}{\partial z}\pm\frac{\partial}{\partial x}\frac{\partial}{\partial y}\frac{\partial M(x,y,z,t)}{\partial z}. \quad (9)$$

Here C is the concentration of the component; t is time; K_x, K_y and K_z are the diffusion coefficients in the x, y and z directions; u, v and w are the velocity components in the x, y and z directions; and M is a quantity which expresses the change in the concentration due to inflow load, settling, deposition, biological and chemical processes.

We used the primary ecological model that was basically developed by the United States Environmental Protection Agency for Chesapeake Bay. This model includes 10 elements, which are shown in below.

1) Phytoplankton (p.p.) carbon (P_c)

$\partial(P_c)/\partial t=$ (P_c increase by p.p. growth) − (Oxidation of organic carbon by p.p. respiration) − (p.p. death) + (p.p. sinking) + (p.p. advection and diffusion) (10)

2) Dissolved organic phosphorus (DOP)

$\partial(\mathrm{DOP})/\partial t=$ (p.p. recycle to DOP by p.p. respiration and death) − (DOP mineralization) − (DOP advection and diffusion) (11)

3) Particulate organic phosphorus (POP)

$\partial(\mathrm{POP})/\partial t=$ (p.p. recycle to POP by p.p. respiration and death) − (POP mineralization) + (POP sinking) + (POP advection and diffusion) (12)

4) Dissolved inorganic phosphorus (DIP)

$\partial(\mathrm{DIP})/\partial t=$ (p.p. recycle to DIP by p.p. respiration and death) + (DOP mineralization) + (POP recycle to DIP by POP mineralization) − (DIP uptake by p.p. growth) + (DIP elution from the sediment) + (DIP advection and diffusion) (13)

5) Dissolved organic nitrogen (DON)

$\partial(\mathrm{DON})/\partial t=$ (p.p. recycle to DON by p.p. respiration and death) − (DON mineralization) + (DON advection and diffusion) (14)

6) Particulate organic nitrogen (PON)

$\partial(\mathrm{PON})/\partial t=$ (p.p. recycle to PON by p.p. respiration and death) − (PON mineralization) + (PON sinking) + (PON advection and diffusion) (15)

7) Ammonia nitrogen (NH_4)

$\partial(NH_4)/\partial t=$ (p.p. recycle to NH_4 by p.p. respiration and death) + (DON mineralization) + (PON mineralization) − (NH_4 uptake by p.p. growth) − (NH_4 nitrification to NO_3) + (NH_4 elution from the sediment) + (NH_4 advection and diffusion) (16)

8) Nitrogen as nitrate and nitrite (NO_2+NO_3 : NO_{23})

$\partial(NO_{23})/\partial t=$ (NH_4 nitrification to NO_{23}) − (NO_{23} uptake by p.p. growth) + (NO_{23} elution from the sediment) + (NO_{23} advection and diffusion) (17)

9) Carbonaceous biochemical oxygen demand (CBOD)

$\partial(\mathrm{CBOD})/\partial t=$ (CBOD production by p.p. death) − (CBOD decay by oxidation of organic materials) + (CBOD inputs from the sediment) + (CBOD advection and diffusion) (18)

Table 1. Flow calculation condition

Item	value
Horizontal grid	50m to 1000m transformed grid
Vertical grid	1m to 5.2m transformed grid
Initial Temperature	Observed average distribution
Initial Salinity	Observed average distribution
Horizontal eddy viscosity	Transformed value (Smagorinsky scheme)
Vertical eddy viscosity	10^{-3} (m^2sec^{-1})
Horizontal eddy diffusivity	1/5 of Horizontal eddy viscosity
Vertical eddy diffusivity	10^{-5} (m^2sec^{-1})
Tide level change	55.3cm at boundary (M_2 tide)
Yahagi River run off	$56.47m^3sec^{-1}$
Toyokawa River run off	$46.30m^3sec^{-1}$
Temperature of river water	Calculation Temp. of run off cell
Salinity of river water	Yahagi R.; 16.8 psu, Toyokawa R.; 17.6 psu
Meteorological condition	Observed average value by Nagoya,Tsu and Irako weather stations
Calculation period	20 cycles of M_2 tide

10) Dissolved oxygen (DO).

$\partial(\mathrm{DO})/\partial t$ = (DO production by photosynthesis) − (DO loss by p.p. respiration) + (DO input by aeration) + (DO loss by nitrification) − (DO loss by oxidation of organic carbon) − (DO loss by sediment oxygen demand) + (DO advection and diffusion) (19)

BOD is also treated in the calculation but since only measured values of COD are available in this region, the calculated values of BOD were converted to COD from the relationship between TOC and COD obtained from the relationship between observed values of TOC and BOD in the inland bay (Japan Environment Agency: 1989 The Oceanographical Society of Japan, 1985) and the model calculation. In this study, the magnification between CBOD and BOD were 1–3 and the relationship between COD and TOC, BOD and COD were as follows.

$$\mathrm{COD} = 1.6\mathrm{TOC} - 0.26 \quad (20)$$

$$\mathrm{BOD} = 3(0.56\mathrm{COD} - 0.06\mathrm{Chl}\text{-}a + 0.14) \quad (21)$$

Here, $\mathrm{TOC} = \mathrm{Pc} + 1/a_{oc} \times \mathrm{BOD}$, $\mathrm{Pc} = 60/1000 \times$ Chl-a and $1/a_{oc} = 12/32$.

2.4 Boundary conditions of the water quality model

At the sea surface and the bottom, $\partial C/\partial z = 0$. At the boundary with land, $\partial C/\partial l = 0$. Here C is concentration of water quality. l is the normal direction toward the boundary. The water quality at the open boundary is adjusted to the value of the open ocean when it is inflow, and when it is outflow, the second derivatives are assumed to be zero. At the sea surface, sunlight intensity is given for photosynthesis. At the sea bottom, there is nutrients elusion from bottom mud. The other boundary conditions used for the water quality calculation follow those used for the flow calculation.

3. Results of flow calculation

3.1 Flow calculation conditions

The initial density distribution was given based on data observed by the Aichi Prefectural Fisheries Experiment Station from 1979 to 1984 and by the Aichi Prefecture Environment Department from 1979 to 1988. The river inflow data were obtained from the summertime average of measurements made by the River Bureau of the Ministry of Construction. Meteorological conditions were obtained as the averages from 1961 to 1990 of observations by Irako Weather Observatory. The average of the M_2 tides at Irako and Morozaki, 55.3cm, was used as the tide level at the bay mouth. The specifications of the hypothetical power plant were intake of 400 $m^3\,s^{-1}$ of cooling water at the bottom, discharge of the same amount at the surface and temperature increase of 7℃ of cooling water passing through the power plant. Horizontal grid spacings gradually increased from 50m at the outlet of the power plant to

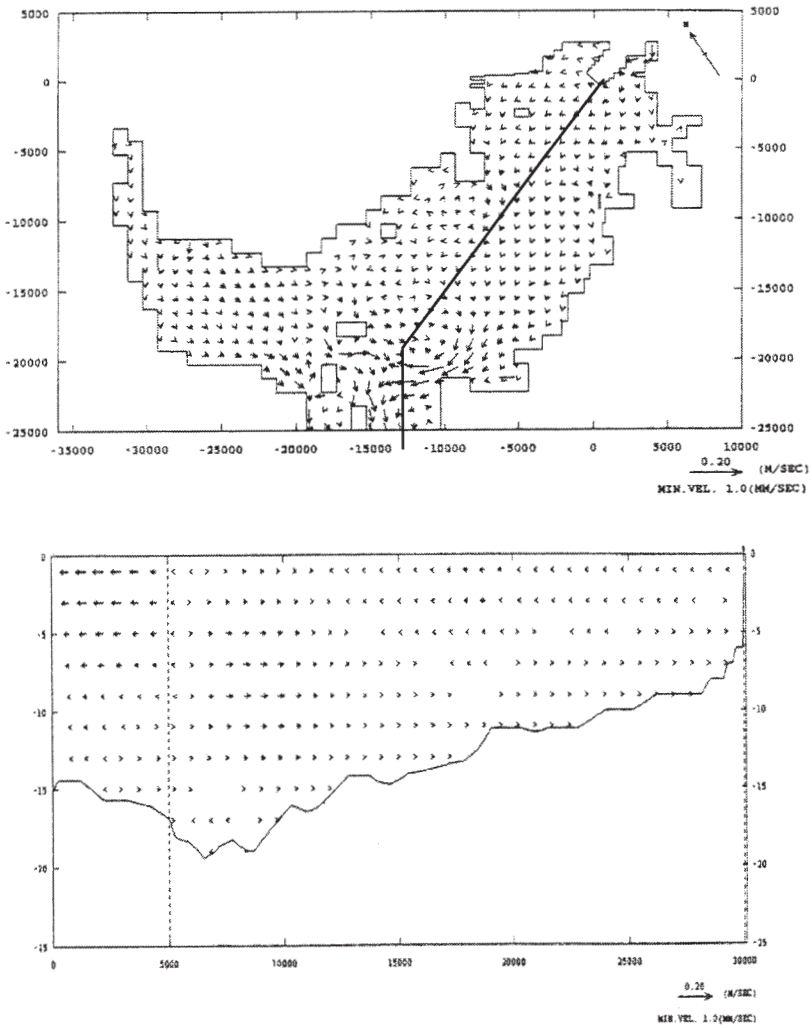

Fig. 2. Distribution of calculated horizontal mean flow and flow pattern of cross section. (Solid line in the upper panel shows the position of cross section below.)

1,000m in open water; there were 20 vertical layers, increasing from 1m thick at the surface to 5.2m thick at the bottom. These conditions are shown in Table 1.

3.2 Results of flow calculation

The mean current in Mikawa Bay was obtained by averaging over the tidal period of calculation in the present state, without a power plant. In most places the mean current was on the order of several cm s^{-1}, but at and around the bay mouth it reached 10cm s^{-1}. The mean current pattern shows outflow at the surface and inflow at the bottom (Fig. 2). This pattern, which is believed to be driven mainly by the density difference, agrees well with the summer mean current obtained from 15 days of continuous observation (Fig. 3). The tidal ellipse of numerical calculation agrees well with the observed M_2 tidal ellipse in axial direction and amplitude (Fig. 4).

From the difference between the mean currents at present and in the case with a hypothetical power plant installed, shown in Fig. 5, it is seen that the effect of the power plant discharge extends out horizontally from the

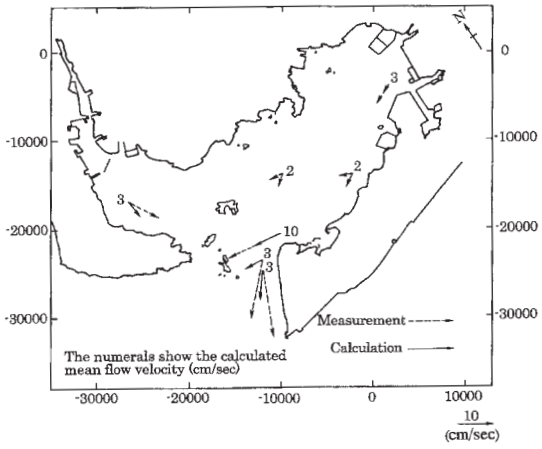

Fig. 3. Comparison of calculated mean flow and measured flow averaged over the measurement period.

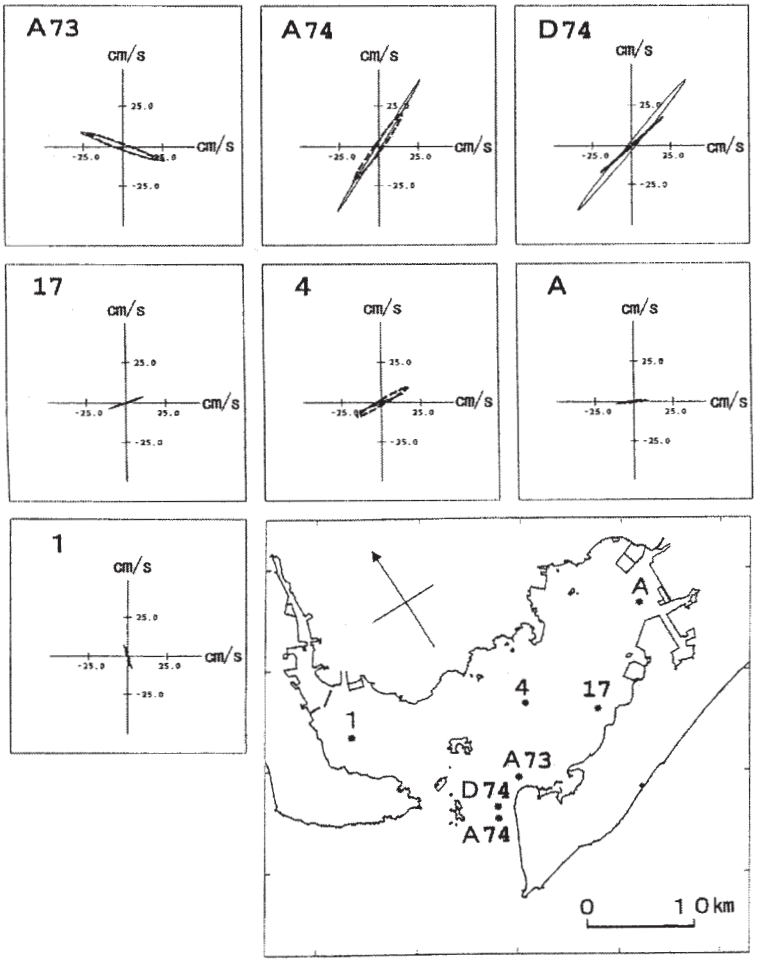

Fig. 4. Comparison of measured and calculated M_2 tidal ellipses. Solid lines: Measurements. Broken lines: Calculations.

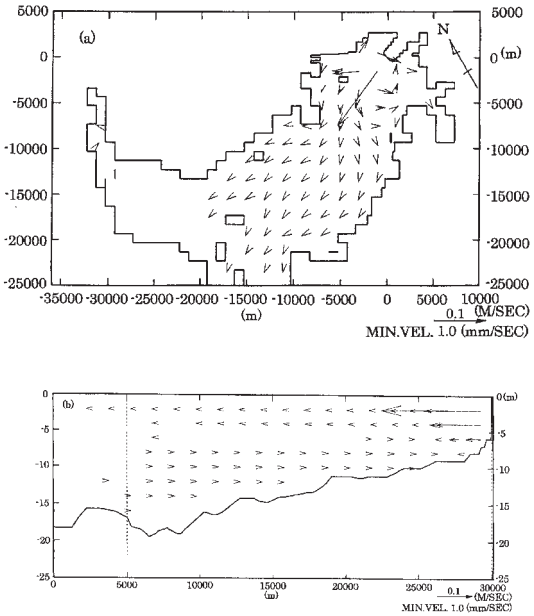

Fig. 5. Differences between the present flow and after construction of a hypothetical power plant.

discharge outlet, and vertically to a depth of 5m. It was found also that both the outflow from the bay in the upper layer and the inflow in the lower layer increased due to the intake and discharge. The effect of power plant discharge(UNOKI, 1998) is further shown by comparisons of the flow with and without discharge across cross sections in the bay interior and at the bay mouth in Fig. 6. In the bay interior, the lower layer inflow increases from 225 $m^3 s^{-1}$ without the discharge to 424 $m^3 s^{-1}$ with the discharge.

The increase corresponds to 50% of the amount of the discharge. In the cross section at the bay mouth, 27 km from the discharge outlet, the inflow increases about 40 $m^3 s^{-1}$, from 1316 $m^3 s^{-1}$ without the discharge to 1354 $m^3 s^{-1}$ with the discharge. This corresponds to 10% of the amount of the discharge and 3% of the inflow at the bay mouth, and is significant compared to the estimated error of 0.3% (Table 2) in the calculated inflow and outflow.

4 Water quality calculation

4.1 Calculation conditions

July average values computed from observations from 1979 to 1984 by the Aichi Prefectural Fisheries Experiment Station and from 1979 to 1988 by the Aichi Prefecture Environment Department were used as initial conditions for the water quality variables. Results of calculations without a power plant were compared against averages of observed values in August. The values calculated by the Aichi Prefecture Environment Department (1994) were used for the river load. Since the Irako Weather Observatory does not observe sunlight intensity or percentage of possible sunshine, averages of values observed from 1961 to 1990 by the Nagoya District Meteorological Observatory were used.

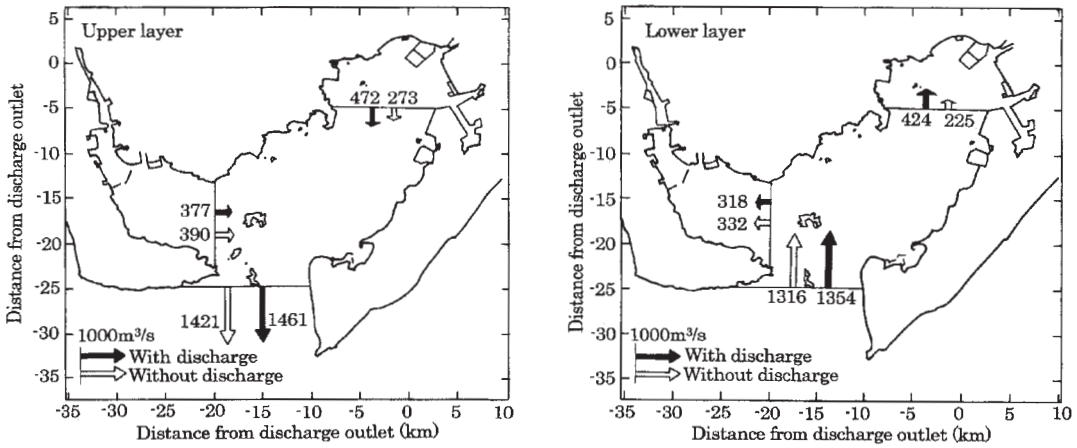

Fig. 6. Comparison of inflow and outflow rates at present and after construction of a hypothetical power plant.

Table 2. Inflow and outflow water volume through the Bay mouth and volume error of flow calculation

	Outflow (m^3/s)	Inflow (m^3/s)	Volume gap (m^3/s)	River run off (m^3/s)	Volume error (m^3/s)	Volume error/Inflow (%)
Without discharge	1421	1316	105	103	2	0.2
With discharge	1461	1354	107	103	4	0.3

Table 3. Water quality calculation condition

Item	value
Water Temp.	Result of heat diffusion calculation
Chl-*a*	3 $\mu g/\ell$
COD	Observed minimum value in each layer
Other variables of water quality	Observed average distribution
Toyokawa River load	T-N:5542;T-P:123;COD:7610;DIP:112;DIN:4990 (Kg day^{-1})
Yahagi River load	T-N:4823;T-P:448;COD:15653;DIP:215;DIN:1981 (Kg day^{-1})
NH_4 flux from bottom mud	2.054 (mgN $m^{-2}day^{-1}$)
NO_3 flux from bottom mud	2.054 (mgN $m^{-2}day^{-1}$)
PO_4 flux from bottom mud	0.456 (mgP $m^{-2}day^{-1}$)
Sediment oxygen demand	$SOD=400\times e^{-0.069\cdot T}$ T: water temp.
Sunshine intensity	397.5 (ly day^{-1})
Power plant cooling water volume	400 (m^3sec^{-1})
Δt of cooling water	7 (℃)
Other parameters	Omission

Values given by the Japan Environment Agency (1989) were used for the nutrient elution rate from bottom mud. Elution rate of DIN is 28.75 mg m^{-2} day^{-1} and elution rate of DIP is 14.60 mg m^{-2} day^{-1}. For oxygen consumption rate by bottom mud, we used a function [$SOD=400\times e^{-0.069\cdot T}$; where T is water temperature] given in Aichi Prefecture Environment Department (1994). These conditions are shown in Table 3.

4.2 Results of water quality calculation

Calculated values were compared with average values and standard deviations of water quality variables observed in the bay from 1979 to 1988, and the reproducibility of the results was investigated. The elements that were compared are Chl-*a*, DO and COD. The results of the comparison are shown in Fig. 7.

The calculated values for Chl-*a* in Chita Bay are a little small, but otherwise values for Chl-*a* show good agreement. The calculated values are within the standard deviations of the observed values at 12 to 17 points in the bay. Comparisons were done for DO and COD at 12 points in the bay. There is good agreement for DO at all points, and for COD except in the lower layer at 2 points. These 2 points are located near the calculation boundary; we believe that the effect of the boundary is responsible for the disagreement between these 2 points. Overall the agreement is good, and the water quality calculation gives good reproducibility.

Next, from comparison of water quality calculations before and after installation of the hypothetical power plant, the cause of the water quality change and the effectiveness in improving water quality were analyzed. For all of the water quality elements, the isolines spread out in concentric circles from the discharge outlet. After the water in the bottom layer upwelled and reached the surface, favorable conditions for primary productivity to become active were fulfilled, and as phytoplankton multiplied the water quality steadily changed. The changes in the various water quality elements are shown in Fig. 8. This figure compares the concentrations of these elements before and after installation of the hypothetical power plant along the water discharge axis.

When the water is discharged after having its temperature increased 7℃ as it passed

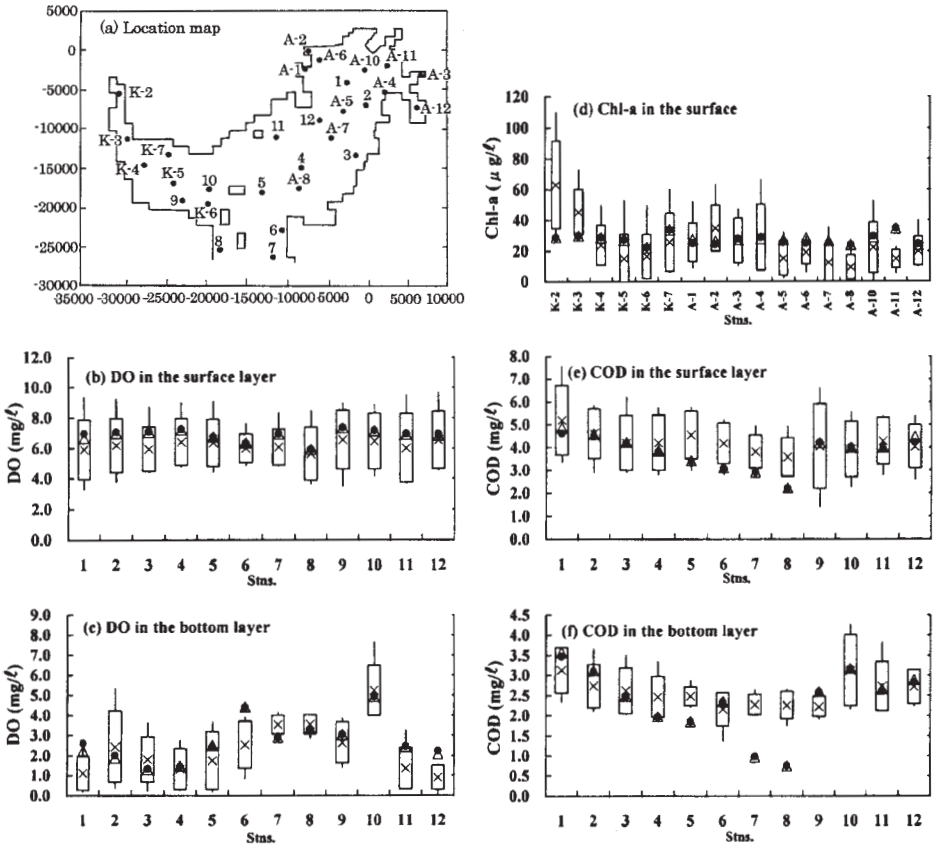

Fig. 7. Comparison between calculated values and observed average values of water quality variables. (● : Calculation value without discharge, △ : Calculation value with discharge, ×: Measured mean value, Box : Standard deviation around mean value, Line : Measured maximum and minimum value.)

through the power plant, the temperature drops to 1℃ 10km offshore.

The discharged cooling water has 2 times the DIN concentration and 1.5 times the DIP concentration compared with the ambient surface water; 6km offshore both are reduced to the levels in the ambient surface water due to consumption by phytoplankton en route. In the case of DIN, beyond 6km consumption by phytoplankton that have multiplied in the heated cooling water outflow exceeds the amount of DIN upwelled from deeper layer, causing the level to drop below the level before installation of the hypothetical power plant. The amount of phytoplankton at the discharge outlet is only 60% of the amount before installation of the hypothetical power plant, but increases rapidly until it exceeds the previous level 3km offshore. The phytoplankton concentration reaches a peak 6km offshore, then decreases gradually to the previous level.

In this calculation, the COD concentration essentially reflects the level of internally productive pollutants, and varies in a manner similar to the Chl-*a* concentration.

DO has a concentration of 3.5mg l^{-1}, 50% of the level before installation of the hypothetical power plant, at the discharge outlet, but due to multiplication of phytoplankton and aeration by 8km offshore it has returned to the previous level.

It is clear from these changes that the principal variations in water quality occur within the limits where the increase in water temperature

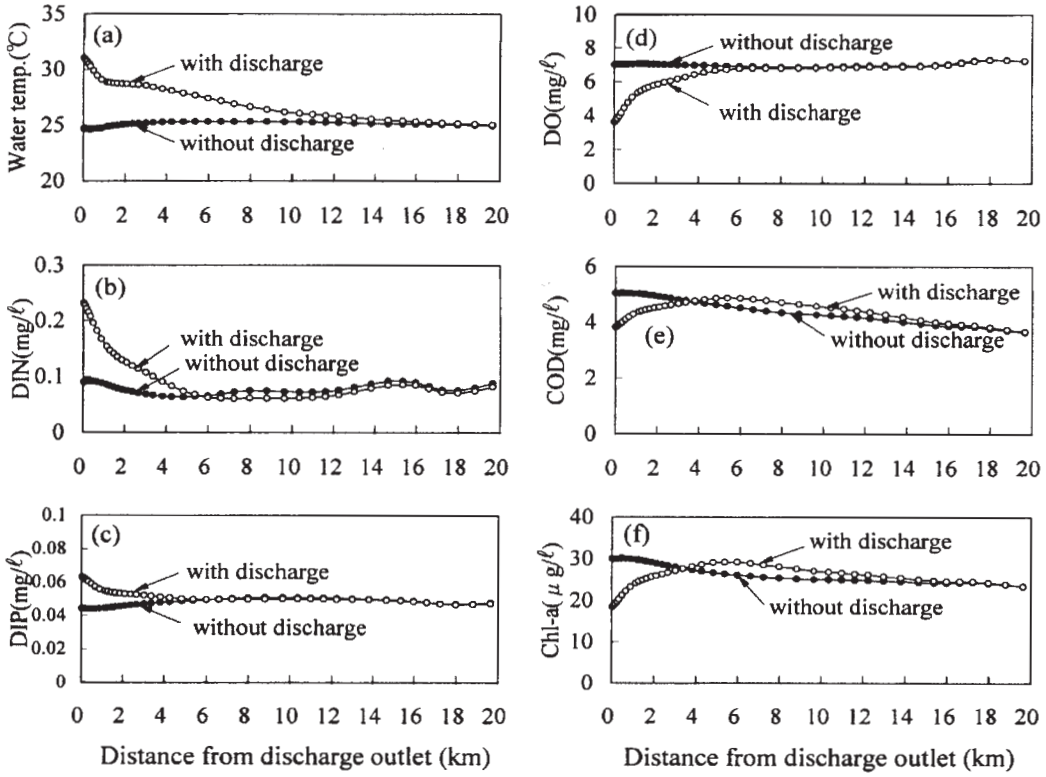

Fig. 8. Comparison of selected water quality concentrations before and after installation of the hypothetical power plant.

Table 4. Comparison of concentrations of selected water quality variables in a crossed section across the bay mouth at present and after construction of the hypothetical power plant.

Upper layer (0 to 9m depth)

	Chl-a (μg/l)	COD (mg/l)	DO (mg/l)	T-N (mg/l)	T-P (mg/l)
①Without discharge	12.2881	2.0996	5.0694	0.6299	0.0914
②With discharge	12.2992	2.107	5.0804	0.6278	0.0912
②−①	0.0111	0.0074	0.011	−0.0021	−0.0002
%	0.1	0.4	0.2	−0.3	−0.2

Lower layer (9 to 25m depth)

	Chl-a (μg/l)	COD (mg/l)	DO (mg/l)	T-N (mg/l)	T-P (mg/l)
①Without discharge	4.8526	1.1061	3.6151	0.6489	0.089
②With discharge	4.7882	1.0947	3.6298	0.6477	0.0887
②−①	−0.0644	−0.0114	0.0147	−0.0012	−0.0003
%	−1.3	−1	0.4	−0.2	−0.3

is 1℃ or greater. Chl-*a* and COD continue to change somewhat a bit farther offshore, but even in these cases the peaks are reached within the area of temperature increase 1℃ or greater.

Next, to investigate the effect of intake and discharge of cooling water on water quality throughout the entire bay, the changes in the average concentrations of water quality elements flowing in and out through a cross-section at the bay mouth were investigated (Table 4). As a result, it was found that after construction of the power station, in the upper layer, where the flow is outward from the bay, the concentrations of Chl-*a*, COD and DO increased, while in the lower layer, where the flow is into the bay, Chl-*a*, COD, T-N and T-P decreased. Accordingly, it appears that there is a net outflow of organic matters out of the bay. T-N and T-P decrease slightly both in the upper and lower layers; further investigation is needed to determine the cause of this (MATSUKAWA, 1993).

5 Summary

The changes in flow and water quality environment in a relatively large scale, nutrient - enriched, closed inland bay, were analyzed quantitatively using a quasi 3-dimensional flow model and a primary ecological model, when a power station is constructed in the innermost of the bay. We investigated how the intake and discharge of cooling water by the power plant would affect seawater exchange and water quality in the closed inland bay.

In this research, we found from the difference between the present flow in the bay and the flow after a hypothetical power plant is installed that, the heated cooling water discharged from the power plant clearly had the effect of increasing the inflow and outflow of sea water into and out of the bay. It is believed that this effect on sea water exchange varies with the amount of discharge water compared to the volume of the bay. Moreover, the location in where the power plant is constructed will also affect the sea water exchange. In the case of Mikawa Bay with a volume of 5.4km^3, the water exchange rate increases 3% at the mouth of the bay if the discharge flow rate is about 400 m^{3}s^{-1}. Since the exchange of sea water at the mouth of Mikawa Bay in summer is about of 1300 m^3 s^{-1}, the effect of the intake and discharge of cooling water is expected to be large in small bays.

We studied the effect of power plant construction on the water quality environment from the calculated difference in water quality between the present and the case in which a power plant is constructed. We showed that there was a tendency for phytoplankton and COD, at high concentrations, to flow out through the bay mouth in the upper layer and, at low concentrations, to flow in through the lower layer, so that the water quality in the bay is improved, as the circulation intensifies. The concentrations of water quality parameters increase and decrease following a typical pattern around the discharge point, but these changes are limited to a relatevely narrow area where the water temperature increase 1℃ or more.

In this study we quantified the effect of a power plant cooling water discharge on the flow and water quality in a bay. It was shown clearly that there was at least a possibility that the water intake and discharge could improve the flow and water quality environment of a closed inland bay.

Acknowledgments

The authors would like to acknowledge the cooperation of Ms. Michiho MORI, Mr. Masakazu MIURA and Mr. Hiroshi INO of Japanese Union Institute of Scientists and Engineers for their assistances in the computational works and data processing. This study was partly supported by the Nuclear and Industrial Safety Agency, Ministry of Economy, Trade and Industry of Japan.

References

Aichi Prefectural Environment Department (1994): Report on 1993, Nutrient Enrichment Model of Ise Bay, 28–40.

Japan Environment Agency (1989): Report on Study of the Mechanism of Marine Pollution in a Closed Inland Bay. 66–68.

MATUKAWA, Y. (1993): Fluctuation and Transport in Mikawa Bay. Bulletin on Coastal Oceanography, **30**, 187–193.

MULLIGAN, T. J. (1987): A steady－state coupled

hydrodynamic/water quality model of the eutrophication and anoxia process in Chesapeake Bay. Hydroqual Inc., 400pp.

SUDO, S. (1993): On acceleration of seawater exchange by the intake of water by a power plant. Marine Ecology Research Institute News, **41**, 2–3.

The Oceanographical Society of Japan (1985): Methods of Investigating the Oceanic Environment. 7. Chemical Research, 7.5.2 TOC and DOC. Koseisha Kosei Kaku Co., Ltd., Tokyo, 291–300.

UNOKI, S. (1998): Relation between the Transport of Gravitation and River Discharge in Bays. Oceanography in Japan, **7**, 283–292.

UNOKI, S. (1978): Oceanographic Description of the Coast of Japan XV: Ise and Mikawa Bays (II), the physical environments. Bulletin on Coastal Oceanography, **15**, 143–154

Received February 14, 2002
Accepted December 9, 2002

La mer 40 : 203, 2002
Société franco-japonaise d'océanographie, Tokyo

資　料

第 40 巻第 4 号掲載欧文論文要旨

ナルジャマン・スザンナ* 柳　哲雄：インドネシア・ジャカルタ湾の低次生態系**

インドネシア・ジャカルタ湾の雨季と乾季の低次生態系の特性を観測データと数値生態系モデルにより調べた。乾季より雨季の方が高いという，観測されたクロロフィル-*a*（Chl-*a*）濃度と溶存態無機窒素（DIN）濃度の季節変動は，1次元の数値生態系モデルによりよく再現された。ジャカルタ湾の基礎生産は416–830mgC/m^2/dayで，この湾が中栄養状態にあることを示している。また，ジャカルタ湾では新生産と再生生産の比は1.0で，陸からのDIN負荷と再生DINがともに chl-*a* 濃度を上昇させることに貢献している。

（*九州大学大学院総合理工学府大気海洋システム学専攻 〒816–8580 春日市春日公園 6－1　**九州大学応用力学研究所 〒816–8580 春日市春日公園 6－1）

前川陽一* 内田　誠* 吉田昭三 永田　豊**：黒潮大蛇行内側に発生した厚い安定した暖水渦**

2000年1月から2001年10月の間，本州南岸を流れる黒潮流は大蛇行路をとっていた。しかし，流路はしばしばW型を示し，時空間共に変動性に富んでいた。この期間内に，2度にわたり，継続時間が約200日に及ぶ安定した暖水渦が，大蛇行内側の冷水域に現れた。三重大学生物資源学部所属の練習船勢水丸を派遣して，これらの暖水渦の構造を調べたが，これらの暖水塊は厚く，数百メートルの深さに達しており，また，その内部の水の起源は，黒潮流軸より沖の水であることが示された。（財）日本水路協会海洋情報研究センターが毎週発行している相模湾・伊豆諸島近海海洋速報をもとに暖水渦の消長を調べたが，この2つの暖水渦は伊豆半島沖で生じた黒潮流路のくびれから，西方に伸びた暖水舌から発生していることが分かった。2001年11月以降は，黒潮流路は直進路をとるようになり，それ以後はこのような厚い安定した暖水渦は発生していない。

（*三重大学生物資源学附属練習船勢水丸　〒514–2221　津市高野尾町2072–2　**（財）日本水路協会海洋情報研究センター　〒104–0061　東京都中央区銀座 7 丁目15－4　三島ビル 5 階）

高野泰隆*，柴崎道廣，和田　明***：発電所冷却水による閉鎖性内湾の流動・水質環境改善の可能性について**

日本国内における火力・原子力発電所は，海水を冷却水に使用するため，沿岸に立地している。発電所は海水に流れと温度負荷を与える以外，水質環境影響物質を負荷しないが，環境に対して流動変化や温度変化を通じて 2 次的に影響力を持つと考えられる。

我々は閉鎖性内湾奥部に立地した発電所の温排水取放水が，湾の海水循環と水質環境を改善できる可能性があるのかを，三河湾を対象に，3 次元流動・水質シミュレーションモデルと仮想発電所によって検討した。流動・水質計算の結果は，発電所取放水が湾の海水交換（下層流入，上層流出）を約 3 %増幅させ，これに伴って緩やかな水質改善が起こる可能性が示された。また，発電所放水口前面では，DO，Chl-*a*濃度の低下や栄養塩類濃度の増加など，連続的に汲み上げられる底層水のため，同心円上の水質変化が特徴的に表れる。しかし，これらの変化は曝気や光合成のため，同心円の外側に向かって急速に現状の状態に回復し，有意な水質変化の範囲は温排水により海水温が 1 ℃上昇する範囲を超えなかった。

（*（株）水圏科学コンサルタント　〒145–0064　東京都大田区上池台1–14–1　**（財）海洋生物環境研究所　〒101–0051　東京都千代田区神田神保町3–29　***日本大学　生産工学部　〒275–8575　千葉県習志野市泉町1–2–1）

La mer 40: 204–209, 2002
Société franco-japonaise d'océanographie, Tokyo

学 会 記 事

1. 2002年 9 月27日(金)東京水産大学海洋環境棟会議室において第 1 回 幹事会が開かれた。会の活性化をはかるための会長の原案が披露された。
主な審議事項は，学会ホームページの作成，編集委員会の委員や構成，会員の増大を計る方策などで，結論までには至らなかった。

2. 2002年11月21日(金)平成15年度科学研究費助成金の申請書を提出した。

3. 2002年11月27日(木)東京水産大学海洋環境棟会議室において第 2 回 幹事会が開かれた。編集状況，ホームページの進捗状況が報告され再度会員の増大を計る方策を検討した。引き続き，学会賞受賞候補者推薦委員会が開かれ，委員長に山口征矢会員が選出された。

4. 2003年 2 月 7 日(金)第19期学術会議会員選出候補者の推薦依頼状を各評議員に送付した。

5. 新入会員

氏 名	所属・住所等	紹介者
山崎紗衣子	東京水産大学 神鷹丸 〒108-8477 港区港南4-5-7	森永 勤
木下 泉	高知大学海洋生物教育センター 〒781-1164 土佐市宇佐町井尻194	河野 博
日下 啓作	宮城県気仙沼水産試験場 〒988-0247 気仙沼市波路上沼119	荒川久幸

6. 退会(逝去者含)
辻田時美　　岡田 操

7. 受贈図書
広島日仏協会報 No. 157，158
なつしま No. 198〜No. 204
東海大学紀要 54号 55号
東海大学海洋研究所研究報告 24号
農業工学研究所ニュース(22，23)
年報(14)
NII News No. 12，13，14
NTT R&D Vol. 51(10，11，12)，52(1，2，3)
養殖研ニュース No. 50
勇魚 No. 26
水産総合研究センター広報 No. 3，4，5
九州大学応用力学研究所 研究論文抄録集 1999年，2001年
応用力学研究所要覧 No. 29
Reports of Research Institute for Applied Mechanics Kyushu University No. 119，120
RESTEC 50号
Journal of Ocean University of Qingdao Vol. 1(1)
Journal of the Korean Society of Oceanography Vol. 37(3，4)
Ocean and Polar Research Vol. 37(3，4)
青島海洋大学学報(自然科学報) 第31巻(3，4，5，6) 第32巻(1，2，3，4)
海洋与湖沼 Vol. 33 (5，6)

日仏海洋学会誌「うみ」投稿規定

1.「うみ」（欧文誌名 La mer）は日仏海洋学会の機関誌として，和文または欧文により，海洋学および水産学ならびにそれらの関連分野の研究成果を発表する学術雑誌であり，同時に研究者間の情報交換の役割をもつことを目的としている。

2.「うみ」は，原則として年 4 回発行され，投稿（依頼原稿を含む）による原著論文，原著短報，総説，学術資料，書評その他を，編集委員会の審査により掲載する。これらの著作権は日仏海洋学会に帰属する。

3. 投稿は，日仏海洋学会会員，および日仏海洋学会正会員に準ずる非会員からとする。共著者に会員を含む場合は会員からの投稿とみなす。

4. 用語は日，仏，英 3 か国語のいずれかとする。ただし，表および図説明の用語は仏文または英文に限る。原著論文には約200語の英文または仏文の要旨を別紙として必ず添える。なお，欧文論文には約500字の和文要旨も添える。ただし，日本語圏外からの投稿の和文要旨については編集委員会の責任とする。

5. 原稿はすべてワードプロセッサを用いて作成し，本文・原図とも 2 通（正，副各 1 通）ずつとする。副本は複写でよい。本文原稿はすべてA4判とし，白紙にダブル・スペース（和文ワープロでは相当間隔）で記入する。表原稿および図の説明原稿は本文原稿とは別紙とする。

6. 投稿原稿の体裁形式は「うみ」最近号掲載論文のそれに従う。著者名は略記しない。記号略号の表記は編集委員会の基準に従う。引用文献の表示形式は，雑誌論文，単行本分載論文（単行本の一部引用も含む），単行本などの別による基準に従う。

7. 原図は版下用として鮮明で，縮尺（版幅または1/2版幅）に耐えられるものとする。

8. 初校に限り著者の校正を受ける。

9. 会員に対しては 7 印刷ページまでの掲載を無料とする。会員の投稿で上記限度を超える分および非会員投稿（依頼原稿を除く）の印刷実費はすべて著者負担（10,000円/ページ）とする。ただし，カラー印刷を含む場合などには，別に所定の費用を著者（会員，非会員とも）負担とする。

10. すべての投稿原稿について，1 編あたり別刷り50部を無料で請求できる。50部を超える分は請求により50部単位で有料で作製される。別刷り請求用紙は初稿校正と同時に送付される。

11. 原稿の送り先は下記の通りとする。なお著者（共著の場合は代表者）連絡先のe-mailアドレス並びにFAX番号を付けることとする。

〒108–8477 港区港南4–5–7 東京水産大学海洋環境学科（吉田 次郎気付）
日仏海洋学会編集委員会
e-mail : jiroy@tokyo-u-fish.ac.jp

執 筆 要 領

1. 原稿

⑴ 和文原稿の場合：ワードプロセッサを使用し，A4判の用紙におよそ横30字，縦25行を目安に作成すること。

⑵ 欧文原稿の場合：ワードプロセッサを使用し，A4判の用紙にダブルスペース25行でタイプし，十分な英文添削または仏文添削を経て提出すること。

⑶ 和文原稿，欧文原稿いずれの場合も，要旨，表原稿および図版説明原稿はそれぞれ本文原稿とは別紙とする。

⑷ 最終原稿提出の際に，印刷原稿とともに原稿，表，図版が保存されたフロッピーディスク，CD-R/RW，MO等での提出を依頼する。この場合，原稿はMicrosoft WORD，Just System一太郎，PDFの原稿のみに限る。また，表，図版はこれら原稿ファイルの中に取り込むか，bmp，jpg等の一般的な画像ファイルに保存したものに限る。なお，電子媒体は返却しない。

2. 論文記載の順序

⑴ 原著（和文原稿）：原稿の第 1 ページ目に表題，著者名，研究の行われた所属機関，所在地，郵便番号を和文と欧文で記載する。研究終了後所属機関が変わった場合は現所属機関も記載する。連絡先（共著の場合は連絡先

とする著者を明示する）の住所，電話番号，ファックス番号，E-mailアドレスも記す。最後にキーワード（4語以内），ランニングヘッドを英文で記載すること。第2ページ目に欧文要旨（欧文表題，著者名を含む）を200語以内で記す。本文は第3ページ目から，「緒言」「資料」「結果」「考察」「謝辞」「文献」「図版の説明」などの章立てあるいは項目順に記載する。基本的には最近号掲載論文の体裁形式を参考にして投稿原稿を作成すること。原稿には通しのページ番号を記入すること。

⑵ 原著（欧文原稿）：原稿の第1ページ目に表題，著者名，研究の行われた所属機関，所在地，郵便番号を記載する。研究終了後所属機関が変わった場合は現所属機関も記載する。最後にキーワード（4語以内），ランニングヘッドを記載すること。第2ページ目に欧文要旨（欧文表題，著者名を含む）を200語以内で記す。本文は第3ページ目からとする。「Introduction」「Data」「Results」「Discussion」「Acknowledgement」「References」「Figure Caption」などの章立てで順に記載する。基本的には投稿原稿の体裁形式は最近号掲載論文を参考にして作成すること。最終ページに和文の表題，著者名，連絡先著者住所，電話番号，ファックス番号，E-mailアドレスおよび約500字以内の和文要旨を添える。原稿には通しのページ番号を記入すること。

⑶ 原著短報，総説：和文ならびに欧文原稿とも原著論文に準ずる。

⑷ 学術資料，書評：特に記載に関する規定はないが，すでに掲載されたものを参考にすること。

3. 活字の指定

原稿での活字は10.5pt〜12ptを目安に設定し，英数字は半角フォントを用いること。学名はイタリック，和文原稿での動植物名はカタカナとすること。句読点は（。）および（，）とするが。文献リストでは（.）および（,）を用いること。章節の題目，謝辞，文献などの項目はボールドまたはゴシックとする。

4. 文　献

文献は本文および図表に引用されたものの全てを記載しなければならない。和文論文，欧文論文共に筆頭著者のアルファベット順（同一著者については，単著，共著の順とし，それぞれ発表年の古い順）にまとめ，以下の例に従って記載する。

⑴ 論文の場合

有賀祐勝，前川行幸，横浜康継（1996）：下田湾におけるアラメ群落構造の経年変化．　うみ，**34**，45–52.

Yanagi, T., T. Takao and A. Morimoto (1997): Co-tidal and co-range charts in the South China Sea delived from satellite altimetry data. La mer, **35**, 85–93.

⑵ 単行本分載論文（単行本の一部引用）の場合

村野正昭（1974）：あみ類と近低層プランクトン．海洋学講座10　海洋プランクトン（丸茂隆三編），東京大学出版会，東京，p. 111–128.

Wynne, M. J. (1981): Phaeophyta: Morphology and classification. *In* The Biology of Seeweeds. Lobban, C. S. and M. J. Wynne (eds.), Blackwell Science, Oxford, p. 52–85.

⑶ 単行本の場合

柳　哲雄（1989）：沿岸海洋学―海の中でものはどう動くか―．　恒星社厚生閣，東京，154pp.

Sverdrup, H. U., M. W. Johnson and R. H. Fleming (1942): The Oceans: Their Physics, Chemistry and General Biology. Prentice-Hall, Englewood Cliffs, New York, 1087pp.

⑷ 本文中での文献の引用

本文中での文献の引用方法はすでに発行された雑誌を参考にするが，基本的には次の形式に従う。

①Greve and Parsons(1977)

②(Avian and Sandrin, 1988),

③Yanagi *et al.*(1997)は……（3名以上の共著の場合）

④……示している（例えば，Yanagi *et al.*, 1997）（3名以上の共著の場合）

5. 図，表および写真

⑴ 図，表および写真とその説明はすべて英文または仏文を用いる。

⑵ 図，表はそのまま写真製版用の草稿となるような明瞭なもので，A4版の上質紙に作製したもの（写真は，正

原稿についてもオリジナルとは別にA4版の用紙にコピーしておくことが望ましい）のみを受け付ける。カラー図を希望する場合はその旨明記する。この場合，別に所定の費用を筆者負担とする。

⑶ 写真は光沢平滑印画紙に鮮明に焼き付けたものを受け付ける。カラー写真の印刷を希望する場合はその旨明記する。この場合，別に所定の費用を筆者負担とする。

⑷ 図，表，および写真は刷り上がり時に最大横が14cm，縦が20cm（説明文を含む）以内であることを考慮して作成すること。

⑸ 図（写真を含む）には，Fig. 1，Fig. 2，……のように通し番号をつけ，一つの図中に複数の図を含む場合はFig. 3(a) Fig. 3(b)，……のように指定する。本文中での引用は和文原稿の場合も「Fig. 1にみられるように……」のようにすること。

⑹ 表には，表題の次（表の上のスペース）に説明をつけ，表ごと別紙とし，Table 1，Table 2，……のように通し番号をつけること。

⑺ 図，表，および写真は１枚ごとに著者名，通し番号をつけること。また，本文中での挿入箇所を最終提出原稿の該当箇所右欄外に朱書きすること。

⑻ 図，写真の説明は別紙にまとめること。

⑼ 地図にはかならず方位と縮尺または緯度，経度を入れること。

6. 単位

原則としてSI単位を用いること。塩分は実用塩分単位（Practical Salinity Unit:psu またはPSU）を用いる場合は単位なしとする。

Information for Contributors

1. The scientific journal,"La mer,"the official organ of Japanese-French Oceanographic Society (JFOS), is published quarterly. "La mer"is open to all researchers in oceanography, fisheries and related sciences in the world. The journal is devoted to the publication of original articles, short contributions, reviews, book reviews, and information in oceanography, fisheries and related fields. Submission of a manuscript will imply that it has not been published or accepted for publication elsewhere. The editorial board decides the acceptance of the manuscript on the basis of peer-reviews and is responsible for its final editing. The Society reserves the copyright of all articles in the Journal.
2. *Submission*: Manuscripts must be written in French, English or Japanese. Authors are requested to submit their original manuscript and figures with one copy to the Editor in chief.
3. *Publication charges:* For members, there will be no page charge for less than eight printed pages and 10,000 yen will be charged per page for the excess, except for color pages. For nonmembers there is publication charge of 10,000 yen per printed page except for color pages. Color illustrations will be provided at cost.
4. *Proofs and reprints:* Fifty reprints of each article will be provided free of charge. Additional reprints can be provided in blocks of 50 copies. Proofs will be sent to the corresponding author. A reprint order form will be sent with the proofs.
5. Manuscripts should be sent to
   Editor in Chief of "La mer"
   Jiro Yoshida
   Department of Ocean Sciences
   Tokyo University of Fisheries
   Konan, Minato-Ku, Tokyo, Japan 108–8477

Manuscript Preparation

1. General
   1) Manuscripts must be typed with double-spacing on one side of A4 size white paper with wide margins.
   2) Figures, tables, and figure captions should be preparaed separate from the main text.
   3) Authors should submit an electronic copy of their paper with the final version of the manuscript. The electronic copy should match the hardcopy exactly and should be stored in CD-R/W or FD. MS-WORD(Windows) and PDF formats are accepted.
2. Details
   1) The first page of the manuscript should include the title, author's full names and affiliations including Fax numbers and E-mail addresses. The corresponding author should be designated. Key words(up to four words)and running head should be written at the bottom of the page.
   2) An abstract of 200 words or less in English or French should be on the second page.
   3) The main text should start on the third page. Please adhere to the following order of presentation: main text, acknowledgements, appendices, references, figure captions, tables. All pages except the first page must be numbered in sequence.
   4) Mathematical formulae should be written with a wide space above and below each line. Système International(SI)units and symbols are preferred.
   5) All references quoted in the text sohuld be listed separately in alphabetical order according to the first author's last name. Citations mus be complete according to the following examples:
   Article: YANAGI, T., T. TAKAO and A. MORIMOTO(1997): Co-tidal and co-range charts in the South China Sea derived from satellite altimetry data. La mer, **35**, 85–93
   Chapter: WYNNE, M. J. (1981): Pheaophyta: Morphology and classification. *In* the Biology of Seaweeds.

LOBBAN, C. S. and M. J. WYNNE(eds.), Blackwell Science, Oxford, p. 52–85.
Book: SVERDRUP, H. U., M. W. JOHNSON and R. H. FLEMING(1942): The Oceans: Their Physics, Chemistry and General Biology. Prentice-Hall, Englewood Cliffs, New York, 1087pp.

6) *Illustrations*: All illustrations should be provided in camera-ready form, suitable for reproduction(which may include reduction) without retouching. Photographs, charts and diagrams are all to be referred to as "Fig(s)." and should be numbered consecutively in the order to which they are referred. They should accompany the manuscript, but should not be included within the text. All figures should be clearly marked on the back with the figure number and the author's name. All figures are to have a caption. Captions should be supplied on a separate sheet.
7) *Photographs*: Orginal photographs must be supplied as they are to be reproduced(e.g. black and white or color). If necessary, a scale should be marked on the photograph. Please note that photocopies of photographs are not acceptable. Half-tone illustrations should be kept to a minimum.
8) *Color illustrations*: The printing cost of color illistration must be borne by authors or their institution. Authors will recieve information about the cost on acceptance of the manuscript.
9) *Tables*: Tables should be numbered consecutively and given a suitable caption on top and each table typed on a separate sheet.

La mer (Bulletin de la Société franco-japonaise d'océanographie)
Tome 40 (2002)

Sommaire

Numéro 1

Numéro 2

うみ（日仏海洋学会誌）
第40巻（2002年）

総　目　次

第1号

第2号

Numéro 3

Numéro 4

第 3 号

第 4 号

賛 助 会 員

ア レ ッ ク 電 子 株 式 会 社	神戸市西区井吹台東町７－２－３
株式会社 イ ー エ ム エ ス	神戸市中央区多聞通３－２－９
有限会社 英 和 出 版 印 刷	文京区千駄木４－20－６
株式会社 内田老鶴圃 内田 悟	文京区大塚３－34－３
財団法人 海洋生物環境研究所	千代田区神田神保町３－29 帝国書院ビル５Ｆ
株式会社 川 合 海 苔 店	大田区大森本町２－31－８
ケー・エンジニアリング株式会社	台東区浅草橋５－14－10
国 土 環 境 株 式 会 社	横浜市都筑区早渕２－２－２
三 洋 測 器 株 式 会 社	渋谷区恵比須南１－２－８
株 式 会 社 高 岡 屋	台東区上野６－７－22
テ ラ 株 式 会 社	世田谷区代沢４－44－２ 下北沢ビル２Ｆ
日 本 海 洋 株 式 会 社	北区栄町９－２
渡 邊 機 開 工 業 株 式 会 社	愛知県渥美郡田原町神戸大坪230

日仏海洋学会入会申込書

（正会員・学生会員）

	年度より入会	年　月　日申込
氏　名 ローマ字		年　月　日　生
住　所　〒 勤務先　機関名 電　話		
自　宅　住　所　〒 電　話		
紹介会員氏名		
送付金額　円	送金方法	
会誌の送り先（希望する方に○をつける）	勤務先　自　宅	

（以下は学会事務局用）

受付	名簿 原簿	会費 原簿	あて名 カード	学会 記事

入会申込書送付先：〒150-0013 東京都渋谷区恵比寿 3-9-25

（財）日仏会館内

日 仏 海 洋 学 会

郵便振替番号：00150−7−96503